

Counterfactually Fair Reinforcement Learning via Sequential Data Preprocessing

Jitao Wang^{1,a}, Chengchun Shi^{2,b}, John D. Piette^{3,c},
 Joshua R. Loftus^{2,d}, Donglin Zeng^{1,e}, Zhenke Wu^{1,f}

¹Department of Biostatistics, University of Michigan, USA

²Department of Statistics, London School of Economics, UK

³Department of Health Behavior and Health Equity,
 School of Public Health, University of Michigan, USA

^ajitwang@umich.edu, ^bc.shi7@lse.ac.uk, ^cjpiette@umich.edu,

^dj.r.loftus@lse.ac.uk, ^edzeng@umich.edu, ^fzhenkewu@umich.edu

Abstract

When applied in healthcare, reinforcement learning (RL) seeks to dynamically match the right interventions to subjects to maximize population benefit. However, the learned policy may disproportionately allocate efficacious actions to one subpopulation, creating or exacerbating disparities in other socioeconomically-disadvantaged subgroups. These biases tend to occur in multi-stage decision making and can be self-perpetuating, which if unaccounted for could cause serious unintended consequences that limit access to care or treatment benefit. Counterfactual fairness (CF) offers a promising statistical tool grounded in causal inference to formulate and study fairness. In this paper, we propose a general framework for fair sequential decision making. We theoretically characterize the optimal CF policy and prove its stationarity, which greatly simplifies the search for optimal CF policies by leveraging existing RL algorithms. The theory also motivates a sequential data preprocessing algorithm to achieve CF decision making under an additive noise assumption. We prove and then validate our policy learning approach in controlling unfairness and attaining optimal value through simulations. Analysis of a digital health dataset designed to reduce opioid misuse shows that our proposal greatly enhances fair access to counseling.

Keywords: Counterfactual Fairness, Digital Health, Opioid Misuse, Reinforcement Learning, Sequential Data Preprocessing.

1 Introduction

With the widespread integration of machine learning (ML)-based decision making systems in various sectors of the economy such as banking, education, financial analysis and healthcare, there is a growing focus on the ethical and societal implications of its deployment (Howard & Borenstein 2018, Chouldechova et al. 2018, Mehrabi et al. 2021). The susceptibility of ML algorithms to bias is raising concerns about the potential for discrimination, particularly as it affects already socioeconomically-disadvantaged subgroups (e.g., racial/ethnic minorities or women). For example, in healthcare, automated decision making systems may unfairly allocate treatment resources to specific subpopulations to maximize population-wise long-term benefits, while neglecting the needs of patients already at risk for limited access or poor outcomes. To redress these problems, researchers have proposed the imposition of fairness constraints on decision-making in order to achieve various fairness-related objectives (Hardt et al. 2016, Chouldechova 2017, Yeom & Tschantz 2018, Mehrabi et al. 2021, Black et al. 2022, Corbett-Davies et al. 2023).

The counterfactual fairness (CF, Kusner et al. 2017) adopted in this paper requires that, all else being equal, the distribution of the decisions for an individual be the same had the individual belong to a different group defined by a sensitive attribute (e.g., gender, race). Unlike other fairness definitions, CF offers a solution based on causal reasoning, which lends itself to statistical techniques to eliminate the influence of sensitive attributes on the outcomes (Kusner et al. 2017, Silva 2024). DeDeo (2014) further argued that even the most successful algorithms would fail to make fair judgments without causal reasoning. To illustrate the differences in major existing fairness concepts, consider the following simplified single-stage university admissions example (Wang et al. 2022): a university wants to develop an ML-based decision support system for undergraduate admission. The system makes admission decisions based on an applicant’s information, including entrance exam

score, gender, race/ethnicity, access to prior educational opportunities, where the score may be correlated with the rest of the variables and unmeasured factors like aptitude. Below, we discuss three notions of fairness:

1. *Demographic parity*: If the university were to pursue “demographic parity” with respect to gender, the goal would be to ensure admission of an equal proportion of male and female applicants regardless of entrance exam scores or the student’s aptitude. It only seeks to match the proportion of admission between the groups, regardless of actual qualifications, which can be problematic if one group is genuinely different in terms of the distribution of actual qualifications. It is purely a statistical metric without considering causal mechanisms that lead to differences in the observed data.
2. *Equal opportunity*: If the university were to pursue “equal opportunity” (Hardt et al. 2016) with respect to gender, the goal would be to ensure that truly qualified applicants would be admitted with equal probabilities (i.e., true positive rates) across groups defined by gender. Equal opportunity relies on observational measures and checks statistical parity conditional on the true qualification but does not consider why or how group differences arise, i.e., it does not directly model or reason about causal relationships.
3. *Counterfactual fairness*: CF with respect to gender shifts attention to individual-level and a causal interpretation of fairness. It ensures that the chance of being admitted does not change had their gender been hypothetically switched while keeping all else about the individual’s situation the same. Instead of focusing on matching group-level metrics, CF involves building or assuming a causal model that explains how sensitive attributes influence the individual’s observed features.

This example highlights two key distinctions of CF compared to other fairness definitions:

- 1) CF focuses on individual-level fairness rather than group-level, and 2) it seeks to remove direct and indirect effects of sensitive attributes on decisions, ensuring fairness from

a causal, rather than purely statistical, perspective, by considering fairness in slightly different hypothetical worlds.

Significant progress has been made in achieving CF decision making in single-stage scenarios. However, focusing solely on a single static decision can lead to suboptimal outcomes if it fails to consider the dynamic nature of sequential decision-making processes (Liu et al. 2018, Creager et al. 2020, D’Amour et al. 2020). Reinforcement learning (RL) excels at sequential decision-making applications including fintech (Malibari et al. 2023), traffic light control (Wei et al. 2018), and healthcare (Li et al. 2022, Buçinca et al. 2024), by learning policies that maximize future rewards. Despite its success, integrating CF principles within RL remains an under-explored area (Reuel & Ma 2024). The challenges of applying CF in RL are two-fold. First, unlike static scenarios, sensitive attributes may not only directly affect the current state, but also indirectly influence the current state through its impact on previous states and decisions. Disentangling these direct and indirect effects to ensure CF is a significant challenge. Second, most existing RL algorithms operate under a Markov decision process (MDP) model assumption, under which the optimal policy achieves desirable properties such as Markovian properties and stationarity (Puterman 2014). These properties substantially reduce the search space and simplify the algorithm. It is unclear whether these properties still hold when incorporating CF constraints.

Our work is motivated by the “PowerED” study (Piette et al. 2023). The original study was a randomized controlled trial of patients who were at risk for opioid-related harms (e.g., overdose or addiction) in which investigators evaluated an RL-supported, 12-week digital health intervention designed to prevent those negative outcomes through behavioral counseling of opioid users while conserving scarce counselor time. Specifically, the intervention arm used an RL-based automated decision making system to dynamically assign weekly personalized treatment options based on each patient’s self-reported pain score and opioid use behaviors in the prior week, with the goal of reducing self-reported opioid misuse be-

haviors. Treatment options included i) brief motivational interactive voice response (IVR) call (less than 5 minutes), ii) a longer recorded call (5 to 10 minutes), or iii) a live call with counselor (20 minutes). Comparison-group participants received 12 weeks of standard motivational enhancement via weekly calls with a trained counselor. In this paper, we focus on the RL-supported arm of the trial where an RL agent seeks to intelligently allocate a limited supply of counselors' time (option iii).

There are two ways unfairness could be introduced in an application like the PowerED study if fairness-unaware RL algorithms are used (as they were in this trial). First, by directly including sensitive attributes (e.g., ethnicity and gender) into the set of state variables within the RL model, the learned policy could make biased decisions for those minority groups characterized by the sensitive attributes. For example, patients with similar pain levels but different ethnicities might receive different treatment options if the agent uses ethnicity as a decision factor. Second, even when sensitive attributes are excluded from the state variables to make decisions, the effect of the sensitive attribute upon the state variables may still indirectly influence the agent's decisions. For instance, research indicates that Hispanic Americans, despite experiencing higher pain sensitivity, often report fewer pain conditions due to cultural factors (Hollingshead et al. 2016). This under-reporting may mislead the agent to think that Hispanics are experiencing less pain compared to other subgroups and to assign fewer human counseling (option iii above; more efficacious) to Hispanic patients, creating unfairness. In this paper, we demonstrate that CF provides a promising statistical framework to study fair sequential decisions while controlling for both direct and indirect influences of the sensitive attributes.

Contributions Our work makes four main contributions: (i) Motivated by a real-world digital-health application, the PowerED study, we propose a novel and generalized CF definition that is suitable for the more challenging but ubiquitous dynamic setting in which

RL makes sequential decisions; (ii) We theoretically characterize the class of CF policies and prove the stationarity of the optimal CF policy which greatly simplifies the search and evaluation for optimal CF policies by leveraging existing RL algorithms. (iii) Motivated by the theory, we propose a sequential data preprocessing algorithm designed for optimal CF policy learning under an additive noise assumption. We establish theoretical guarantees that our approach asymptotically controls the level of unfairness and attaining optimal value; (iv) We demonstrate the efficacy of our proposed algorithm in controlling unfairness and attaining optimal value through numerical studies and real data analysis.

Related Work on Fair ML A variety of fairness criteria in ML and their characterizations in the literature have been recently reviewed (Kleinberg et al. 2018, Mehrabi et al. 2021, Barocas et al. 2023, Yang et al. 2024, Caton & Haas 2024). Broadly speaking, ML methods addressing fairness goals can be classified into three categories. *Preprocessing* approaches remove potential bias from the data before training. For example, Kusner et al. (2017), Nabi & Shpitser (2018), Chiappa & Isaac (2019), Salimi et al. (2019), Zuo et al. (2022), Chen et al. (2023) used the causal framework of directed acyclic graph (DAG) to remove unfairness from the training data. Others proposed to preprocess the training data using relabelling and perturbation techniques to balance between underprivileged and privileged instances (Kamiran & Calders 2012, Jiang & Nachum 2020, Wang et al. 2019). *In-processing* methods incorporate fairness metrics directly into the model’s training process, for example by regularization or constrained optimization (Berk et al. 2017, Aghaei et al. 2019, Di Stefano et al. 2020, Viviano & Bradic 2024) or with adversarial approaches (Edwards & Storkey 2015, Beutel et al. 2017, Celis & Keswani 2019). *Post-processing* approaches adjust the model’s predictions after training to ensure fairer outcomes for different groups (Pleiss et al. 2017, Hébert-Johnson et al. 2018, Kim et al. 2019, Wang et al. 2022). Several recent works have explored various approaches to achieve CF in single-stage

scenarios. [Chen et al. \(2023\)](#) proposed an algorithm that removes sensitive information from the training data. [Wang et al. \(2022\)](#) developed a post-processing procedure to make unfair ML models fair. [Kusner et al. \(2017\)](#) and [Zuo et al. \(2022\)](#) considered building ML models that rely only on non-sensitive attributes. [Di Stefano et al. \(2020\)](#) proposed to use regularization by incorporating fairness penalty into the loss function.

Paper organization The remainder of this paper is organized as follows. Section 2 reviews structural causal models, counterfactual inference, and the contextual Markov decision process (CMDP) model. In Section 3, we extend single-stage CF to multi-stage decision making under the framework of CMDP. In Section 4, we characterize the form of (optimal) CF policies when the counterfactuals are known. In Section 5, we propose a sequential data preprocessing algorithm for estimating the counterfactuals. The preprocessed data serve as inputs to any offline RL algorithm for CF policy learning. We then theoretically establish value optimality and asymptotic fairness control of the learned policy in Section 5.1, which are empirically supported by synthetic and semi-synthetic experiments in Section 6. We apply the algorithm to a real-world interventional digital health dataset in Section 7. The paper concludes with a brief discussion on limitations and future directions.

2 Preliminaries

To bring the discussion of fairness into the framework of causal inference, we first give a brief introduction to the definitions of structural causal model (SCM) and counterfactuals. Then we introduce the the framework of CMDP in which we define the CF using the language of SCM (Section 3).

2.1 Structural causal model and counterfactuals

Following Pearl et al. (2000), SCM provides a mathematical framework for modeling causal relationships between variables. An SCM $M = (\mathcal{U}, \mathcal{V}, F)$ consists of a set of observable endogenous variables V , a set of unobserved exogenous variables U and a set of functions F . These functions assign value to each endogenous variable V given its parents $pa(V) \in \mathcal{V}$ and unobserved direct causes U : $V = f_V(pa(V), U)$. U are required to be jointly independent. The structure of M can be depicted by a causal graph, usually in the form of directed acyclic graph (DAG), where $(pa(V), U)$ forms the parent set of V .

In the SCM framework, we define counterfactual inference. Assume $Y \in V$ is the variable of interest. Let Z and U_Y be the parents of Y where $Z \in V$ and $U_Y \in U$; let U_Z be the parent of Z and $U_Z \in U$. By the definition of SCM, Y is fully determined by Z and U_Y through function f_Y , i.e., $Y = f_Y(Z, U_Y)$. Given a realization of $U_Y = u_Y$, suppose we have observed the values of Z and Y , denoted as z and y . Consider a typical counterfactual inference statement: what would be the value of Y had Z taken value z' instead of z given we have observed z and y ? This counterfactual query can be realized through Pearl's do-operator, $do(Z = z')$, which generates an interventional distribution by removing the edges leading into Z in the corresponding DAG and set Z to the value z' . Following the notation in the seminal CF paper (Kusner et al. 2017), we denote it by $Y^{Z \leftarrow z'}(U_Y)$, where " $Z \leftarrow z'$ " represents the $do(Z = z')$ operation and $Y^{Z \leftarrow z'}(U_Y)$ is a deterministic function of Z and U_Y . Figure 1 depicts the difference between SCM and counterfactual inference. It is important to note that while U_Y is not directly observable, we can infer its value from the observed values z and y . This inference of U_Y is essential for computing counterfactuals.

We adhere to a general three-step procedure for counterfactual inference to compute this quantity (please refer to Pearl et al. 2016, for more details): 1. *Abduction*: update $P(U_Y)$ by the observed quantities $Y = y, Z = z$, obtaining $P(U_Y|Y = y, Z = z)$. 2. *Action*:

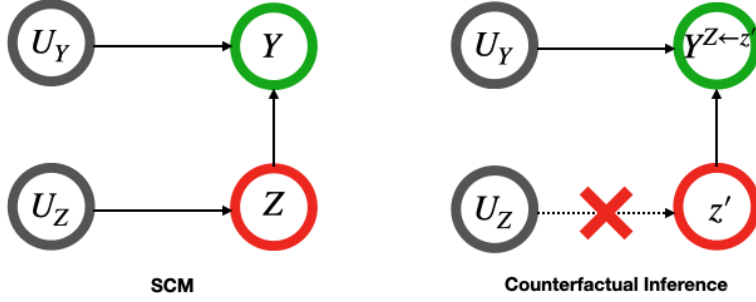


Figure 1: A simple example of SCM and counterfactual inference.

remove the structure equations for Z and replace them with the appropriate value, i.e. $Z = z'$. 3. *Prediction*: use the modified structural model and updated $P(U_Y|Y = y, Z = z)$ to compute $Y^{Z \leftarrow z'}(U_Y)$. We will detail this inference procedure for our specific settings in Section 3.1 and 3.2.

2.2 Contextual Markov Decision Process

Contextual Markov Decision Process (CMDP, [Hallak et al. 2015](#)) is an augmented MDP that incorporates additional contextual information during decision making.

Definition 1 (CMDP). *Contextual Markov decision process is a tuple $(\mathcal{C}, \mathcal{S}, \mathcal{A}, \mathcal{M}(c))$ where \mathcal{C} is called the context space, \mathcal{S} and \mathcal{A} are the state and action space, and \mathcal{M} is function mapping any context $c \in \mathcal{C}$ to an MDP $\mathcal{M}(c) = (P^c, R^c)$.*

We assume the observational data follows a CMDP where the sensitive attributes serve as the contextual information, as illustrated in Figure 2. Consider the collected observed tuples $\{(z_i, s_{it}, a_{it}, r_{it}) : t = 1, \dots, T_i, i = 1, \dots, N\}$, where N denotes the number of subjects and T_i denotes the length of horizons for subject i . For simplicity, we fix $T_i = T$ for all i in the rest of the paper. Z_i denotes time-invariant sensitive attributes for subject i , which takes value from $\mathcal{Z} = \{z^{(1)}, \dots, z^{(K)}\}$. In this paper, we consider the sensitive attributes to be categorical, which is a reasonable assumption for commonly studied attributes such as race and gender. Additionally, for ease of presentation, we focus on a single sensitive

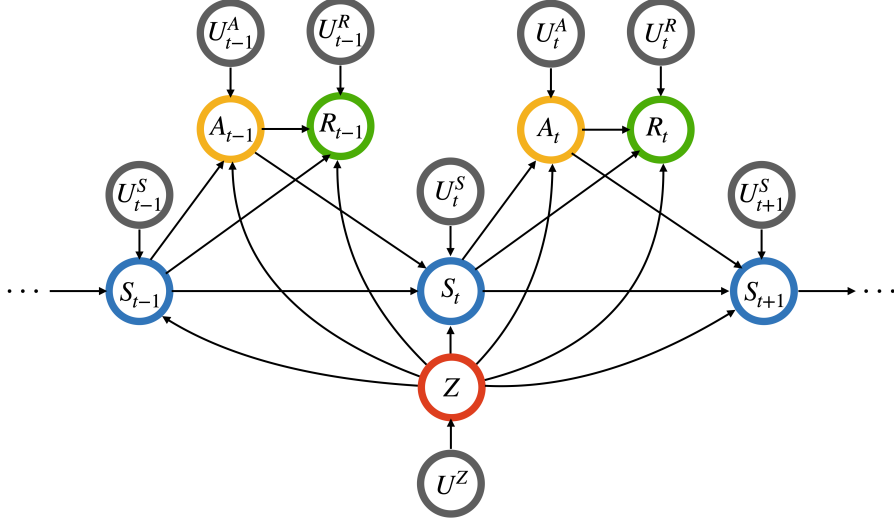


Figure 2: Causal DAG of CMDP.

attribute in this paper, but the extension to multiple attributes is straightforward. For simplicity, we omit index i for individual. Let S_t, A_t, R_t represent the state variables, actions and received reward at time t . U_t^S, U_t^R are the exogenous variables for S_t, R_t . We use $\pi = \{\pi_t\}_{t \geq 1}$ to denote a policy, which consists of a sequence of decision rules. At time t , the environment arrives at a state S_t and the agent takes an action A_t based on a behavior decision rule $\pi_t^{(b)}$ which is specific to the mechanism of how the observed data at hand are collected and often differ from an alternative and potentially better decision rule π_t . The environment then transitions to a new state X_{t+1} and gives a reward R_t according to transition kernel $P_t(S_{t+1}, R_t | S_t, A_t, Z)$. Here the transition kernel P_t can vary by time in general as indicated by the dependence on the index t ; π_t can generally depend on entire history $H_t = \{Z, \bar{S}_t, \bar{A}_{t-1}, \bar{R}_{t-1}\}$ where the notation “ \bar{W}_t ” generically represents the sequence of variable W from time 1 up to and including time t .

We introduce two assumptions as implied by the DAG structure in the CMDP framework and remark on their relevance to our theoretical analyses.

Assumption 1 (No unmeasured confounders). *For each $t < T$, conditional on H_t blocks all backdoor paths from A_t to S_{t+1} and from A_t to R_t .*

Assumption 2 (Markov property). *For any $t < T$, $S_{t+1}, R_t \perp\!\!\!\perp \{S_j, R_{j-1}, A_j\}_{j \leq t-1} \mid S_t, A_t, Z$*

Remark 1. *Assumption 1 ensures that, conditional on the history H_t , there exists no unmeasured confounders between the action A_t and the subsequent state-reward pair (S_{t+1}, R_t) . It is automatically satisfied in our PowerED study where the behavior policy is RL-based and relies solely on patient's observed information. This condition is crucial as it enables consistent estimation of transition and reward functions from observational data. Notably, when this assumption is violated, it may compromise the Markov property, resulting in a confounded partially observable MDP (Lu et al. 2022, Shi, Uehara, Huang & Jiang 2022, Bennett & Kallus 2024, Hong et al. 2024). Assumption 2 implies that the next state S_{t+1} and reward R_t following action A_t are conditionally independent of the entire history given the current state X_t , action A_t , and sensitive attribute Z , making the transition and reward functions only dependent on S_t, A_t, Z rather than the entire history. Consequently, this Markov property enables more efficient policy learning as decisions can be made based on the current state.*

3 Counterfactual Fairness in RL

Before extending single-stage CF (Kusner et al. 2017) to complex CMDP settings, we first consider a simpler contextual bandit setting, which is a simplification of CMDP with only one time step; it helps establish the meanings of notation and the heuristics of why preprocessing strategies can help achieve CF.

3.1 Counterfactual fairness under contextual bandit

Let (Z, X, A, R) be the variables in a contextual bandit setting, as illustrated in Figure 3. Here, Z denotes the sensitive attribute, X represents the non-sensitive context (of dimen-

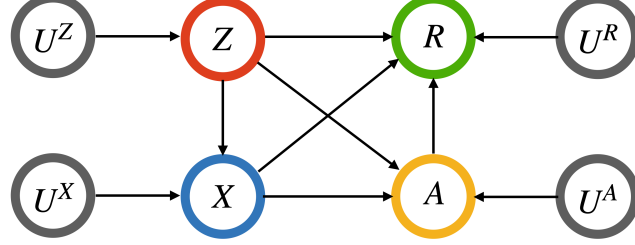


Figure 3: Causal DAG of contextual bandit (one-stage).

sion one for ease of presentation here), A is the action output by the policy, and R is the received reward. Let (U^Z, U^X, U^A, U^R) be the corresponding exogenous variables that determine the values of (Z, X, A, R) , respectively. We adopt the three-step procedure outlined in Section 2.1 to infer the counterfactual context. To ensure well-defined policies that depend on the counterfactual context, we assume that U^X is uniquely determined by x and z . With a slight abuse of notation, we denote by $U^X(\cdot)$ the corresponding mapping function. Without this assumption, this quantity will be a random variable even when conditioned on observed information, resulting in an ill-defined policy. Here we detail the counterfactual inference procedure. We begin by inferring the value of U^X using x and z , i.e., $U^X(x, z)$. Next, we perform the do-operation $do(Z = z')$ by setting the value of Z to z' . Third, based on the inferred $U^X(x, z)$ and intervened z' , we compute the counterfactual context, denoted as $X^{Z \leftarrow z'}(U^X(x, z))$. The counterfactual action $A^{Z \leftarrow z'}(U^X(x, z))$ can be calculated by applying policy π to this counterfactual context $X^{Z \leftarrow z'}(U^X(x, z))$. We formally define CF for a policy π in the contextual bandit framework as follows:

Definition 2 (Counterfactual Fairness in Contextual Bandit). *Given an observed context $X = x, Z = z$, a policy π is counterfactually fair if it satisfies the following equality:*

$$\mathbb{P}^\pi \left(A^{Z \leftarrow z'}(U^X(x, z)) = a \right) = \mathbb{P}^\pi \left(A^{Z \leftarrow z}(U^X(x, z)) = a \right), \quad (1)$$

for any $z' \in \mathcal{Z}$ and $a \in \mathcal{A}$.

To understand this definition, consider an individual with sensitive attribute $Z = z$ who

receives an action $A = a$ according to policy π . CF requires that π must assign the same action a for the same individual, if in a hypothetical world their sensitive attribute Z were changed to any other valid value $z' \in \mathcal{Z}, z' \neq z$.

There are two potential reasons for unfairness to happen if a policy incorporates information from both X and Z . First, inclusion of Z in the policy will make the decisions dependent on the value of Z and thereby introducing potential unfairness. Second, X may also have implicit information about Z because of the causal arrow $Z \rightarrow X$. Even when Z is excluded from being used in a policy, X inherently carries information about Z , potentially leads to unfair decisions. We can remove the potential unfairness introduced by the impact of Z on X via the FLAP algorithm (Chen et al. 2023). For a given tuple (z_i, x_i, a_i, r_i) for individual i , we can remove the influence of z_i from x_i through the following procedure that produces a vector of states under the real and counterfactual worlds: $\tilde{\mathbf{x}}_i = \{x_i - \mathbb{E}_N(X | Z = z_i) + \mathbb{E}_N(X | Z = z)\}_{z \in \mathcal{Z}}$. This preprocessing step generates debiased experience tuples $(\tilde{\mathbf{x}}_i, a_i, r_i)_{i=1, \dots, N}$. $\tilde{\mathbf{x}}_i$ represents the set of all counterfactual states corresponding to all possible values of Z . By construction, $\tilde{\mathbf{x}}_i$ remains invariant across counterfactual values of Z , thereby making the resulting policy not dependent on Z and counterfactually fair. One can then use the preprocessed $(\tilde{\mathbf{x}}_i, a_i, r_i)_{i=1, \dots, N}$ as inputs to any off-the-shelf policy learning algorithm to learn a CF policy under contextual bandits. As we will discuss in Remark 3, this algorithm cannot be directly applied in sequential settings for which our proposal addresses.

3.2 Counterfactual fairness under CMDP

We are ready to generalize the definition of CF from contextual bandit to CMDP settings. Let \bar{U}_t^S and \bar{U}_t^R be the sequence of corresponding noise variables for \bar{S}_t and \bar{R}_t , respectively. The following additional assumption adapted from the contextual bandit settings is needed to ensure that the decision rule π_t is properly defined:

Assumption 3. For any $t > 1$, U_t^S and U_{t-1}^R are deterministic functions of H_t . With a slight abuse of notation, we denote by $U_t^S(\cdot)$ and $U_{t-1}^R(\cdot)$ the corresponding mapping functions, such that: $U_t^S = U_t^S(H_t)$, and $U_{t-1}^R = U_{t-1}^R(H_t)$. Furthermore, let $\bar{U}_t(\cdot)$ be a vector-valued function with component functions: $(U_1^S(\cdot), U_1^R(\cdot), \dots, U_{t-1}^R(\cdot), U_t^S(\cdot))$.

Following Pearl's three-step procedure, we use $A_t^{Z \leftarrow z'}(\bar{U}_t(h_t))$ to denote the counterfactual action that would have been taken following a decision rule π_t for an individual with history h_t had their sensitive attribute been set to z' . With these notation and assumptions established, we can now formally define CF for a decision rule π_t in the CMDP framework,

Definition 3 (Counterfactual Fairness in CMDP). *Given an observed trajectory $H_t = h_t$ where $h_t = \{z, \bar{s}_t, \bar{a}_{t-1}, \bar{r}_{t-1}\}$, a decision rule π_t is counterfactually fair at time t if it satisfies the following condition:*

$$\mathbb{P}^{\pi_t} \left(A_t^{Z \leftarrow z'}(\bar{U}_t(h_t)) = a \right) = \mathbb{P}^{\pi_t} \left(A_t^{Z \leftarrow z}(\bar{U}_t(h_t)) = a \right), \quad (2)$$

for any $z' \in \mathcal{Z}$ and $a \in \mathcal{A}$.

Similar to Definition 2, CF requires that π_t must assign the same action a for the same individual with history h_t , if in a hypothetical world their sensitive attribute Z were changed to any other valid value $z' \in \mathcal{Z}, z' \neq z$, while experiencing the same action sequence \bar{a}_{t-1} . A policy $\pi = \{\pi_t\}_{t \geq 1}$ is said to satisfy CF under CMDPs if each π_t satisfies the Definition 3.

Remark 2. Definition 3 aligns with Pearl's three-step counterfactual inference procedure (Pearl et al. 2016), which we can break down as follows:

- **Abduction step:** \bar{U}_t is the historical values of the background variables that follow the distribution of $P(\bar{U}_t | H_t = h_t)$ that update our knowledge of \bar{U}_t given the observed trajectories h_t ;
- **Action step:** We perform do-operation: Z is set to a hypothetical value z' ;

- **Prediction step:** Based on our updated knowledge of \bar{U}_t given h_t , z' and \bar{a}_{t-1} , we can predict the distribution of A_t following π_t , the decision rule executed by the agent.

4 Characterizing Counterfactually Fair Policies

In this section, we theoretically characterize the class of CF policies under CMDPs, and show the optimal CF policy is stationary when CMDPs are stationary assuming known counterfactual states and rewards. In Section 5, we will present identification assumptions and an algorithm for learning the counterfactual states and rewards from data.

Given the observed history $H_t = h_t$, let \mathcal{S}_t denote the set of counterfactual states at all possible values of Z at time t . Similarly, let \mathcal{R}_t denote the set of counterfactual rewards. Formally, $\mathcal{S}_t = \left\{ S_t^{Z \leftarrow z^{(k)}}(\bar{U}_t(h_t)) \right\}_{k=1,\dots,K}$, and $\mathcal{R}_t = \left\{ R_t^{Z \leftarrow z^{(k)}}(\bar{U}_t(h_{t+1})) \right\}_{k=1,\dots,K}$. In addition, let $\bar{\mathcal{S}}_t = \{\mathcal{S}_{t'}\}_{t' \leq t}$ and $\bar{\mathcal{R}}_t = \{\mathcal{R}_{t'}\}_{t' \leq t}$.

Theorem 1 (Counterfactual augmentation). *Given observed history $H_t = h_t$ under CMDPs, π_t satisfies CF if it admits the following functional form that*

$$\pi_t(\bar{\mathcal{S}}_t, \bar{\mathcal{R}}_{t-1}, \bar{a}_{t-1}), \text{ for any } t. \quad (3)$$

In what follows, we will focus the class of CF policies that take $(\bar{\mathcal{S}}_t, \bar{\mathcal{R}}_{t-1}, \bar{a}_{t-1})$ as input. In DTR settings, the policy that takes observables $(Z, \bar{S}_t, \bar{R}_{t-1}, \bar{A}_{t-1})$ as input would achieve value optimality but violates the CF definition due to its direct use of Z . Our interested policy class of form (3) removes direct or indirect impact of Z in a causal framework, which ensures CF but potentially at the cost of reduced value due to the loss of Z 's information.

In RL, stationarity is often assumed for efficient policy learning (Sutton & Barto 2018). Building on this, we consider stationary CMDPs, where the system dynamics remain invariant over time. A history-dependent policy π is a sequence of decision rules $\pi = \{\pi_t\}_{t \geq 1}$ where each π_t maps $(\bar{\mathcal{S}}_t, \bar{\mathcal{R}}_{t-1}, \bar{a}_{t-1})$ to a probability mass function on \mathcal{A} . When there exists

some function π^* such that $\pi_t(\bar{\mathcal{S}}_t, \bar{\mathcal{R}}_{t-1}, \bar{a}_{t-1}) = \pi^*(\mathcal{S}_t)$ for any $t \geq 1$ almost surely, we refer to π as a stationary policy. Let HCF , SCF denote the class of history-dependent and stationary CF policies, respectively. The following theorem characterizes optimal CF policies under stationary CMDPs.

Theorem 2 (Optimality in stationary CMDPs). *Under a stationary CMDP, there exists some $\pi^{opt} \in SCF$ such that*

$$J(\pi^{opt}) = \sup_{\pi \in HCF} J(\pi),$$

where $J(\pi) = \mathbb{E}_\pi [\sum_{t=0}^{\infty} \gamma^t R_t]$ is integrated expected discounted cumulative reward with discount factor $\gamma \in (0, 1)$.

Theorem 2 implies that the optimal CF policy in a stationary CMDP can be found within the class of SCF , which is much smaller than HCF . Leveraging existing offline RL algorithms with minimal modifications, we can pool information across time to better learn a single stationary policy.

Theorem 1 and 2 suggest that in stationary CMDPs, the optimal CF policy is stationary, where the decisions rely on the most recent counterfactual states at all possible values of Z . However, we can only observe the factual but not the counterfactual states, limiting direct application of these theoretical results. To bridge this gap, we propose a sequential data preprocessing algorithm (Section 5) that estimates these unobserved counterfactuals. This preprocessing step enables the application of existing offline RL algorithms to learn optimal CF policies using the preprocessed experience tuples.

5 Counterfactually Fair Policy Learning

In this section, we focus on the problem of learning optimal CF policies acknowledging that counterfactuals are unobserved. Our proposed approach has two steps. First, we remove

sensitive attribute information from the original dataset via a sequential data preprocessing procedure (Algorithm 1). Second, the preprocessed dataset is used as input to any existing offline RL algorithm to learn the optimal CF policy. Similar to the single-stage setting reviewed in Section 3.1, a key ingredient in the first step is to accurately estimate the counterfactual states and rewards from the observed data at each time point, for which we introduce the following assumption:

Assumption 4 (Additivity). *For all time $t \geq 1$, the exogenous variables U_t^S and U_t^R are additive to S_t and R_t , respectively.*

Assumption 4, which enables the estimation of exogenous variables $\{U_t^S\}_{t \geq 1}$ and $\{U_t^R\}_{t \geq 1}$, allows us to identify and estimate the counterfactual states and rewards using observed data. This assumption is related to *level 3* assumption in Kusner et al. (2017)'s work, which maximizes the information the policy learner can use. Kusner et al. (2017) also introduced *level 1* and *2* assumptions, which are more flexible than this additivity assumption.

With all the necessary assumptions established, we now present Algorithm 1 of the proposed sequential data preprocessing procedure. We use $\hat{s}_{it}(z')$ and $\hat{r}_{it-1}(z')$ to represent the estimated values of $S_t^{Z \leftarrow z'}(\bar{U}_t(H_t))$ and $R_{t-1}^{Z \leftarrow z'}(\bar{U}_t(H_t))$ for individual i , respectively. The algorithm's core strategy is to leverage observed data to estimate counterfactual states and rewards under the additive assumption. These estimates enable us to construct preprocessed experience tuples from the original data, which can then be used to train optimal policies that satisfy CF requirements. Notably, these preprocessed experience tuples naturally form a MDP, as shown in the proof of Theorem 2, allowing us to apply existing RL algorithms directly. It is important to note that the rationale for preprocessing s_{it} and r_{it} differs. According to Theorem 1, pre-processing s_{it} ensures that the learned policy achieves CF and there is no requirement on reward r_{it} . One can use preprocessed \hat{s}_{it} and observed r_{it} to learn a CF policy. However, the purpose of preprocessing r_{it} is to ensure that the

learned policy maximizes the cumulative discounted reward under stationary CMDPs based on Theorem 2.

Algorithm 1 Proposed sequential data preprocessing

Input: Original data $\mathcal{D} = \{(s_{it}, z_i, a_{it}, r_{it}) : i = 1, \dots, N; t = 1, \dots, T\}$.

- 1: Fit the mean of transition kernel $\hat{\mu}(s, a, z)$ by minimizing mean squared error (MSE) on \mathcal{D} .
- 2: Estimate $\hat{\mathbb{E}}(S_1|Z = z)$ and $\hat{P}(Z = z) \forall z' \in \mathcal{Z}$ by the empirical means.
- 3: **for** $i = 1, \dots, N$ **do**
- 4: Calculate $\hat{s}_{i1}^{z'} = s_{i1} - \hat{\mathbb{E}}(S_1|Z = z) + \hat{\mathbb{E}}(S_1|Z = z'), \forall z' \in \mathcal{Z}$.
- 5: Set $\tilde{s}_{i1} = [\hat{s}_{i1}^{z^{(1)}}, \dots, \hat{s}_{i1}^{z^{(K)}}]^\top$.
- 6: **for** $t = 2, \dots, T$ **do**
- 7: $[\hat{s}_{it}^{z'}, \hat{r}_{i,t-1}^{z'}]^\top = [s_{it}, r_{i,t-1}]^\top - \hat{\mu}(s_{i,t-1}, a_{i,t-1}, z_i) + \hat{\mu}(\hat{s}_{i,t-1}^{z'}, a_{i,t-1}, z'), \forall z' \in \mathcal{Z}$.
- 8: $\tilde{s}_{it} = [\hat{s}_{it}^{z^{(1)}}, \dots, \hat{s}_{it}^{z^{(K)}}]^\top$,
- 9: $\tilde{r}_{i,t-1} = \sum_{k=1}^K \hat{P}(Z = z^{(k)}) \hat{r}_{i,t-1}^{z^{(k)}}$.
- 10: **end for**
- 11: **end for**

Output: Preprocessed experience tuples $\{(\tilde{s}_{it}, a_{it}, \tilde{r}_{it}) : i = 1, \dots, N; t = 1, \dots, T\}$.

Remark 3. Algorithm 1 generalizes the data preprocessing algorithm in Chen et al. (2023), which shares the idea of estimating the counterfactual states through preprocessing. Although their approach can be extended to single-stage contextual bandit settings, it falls short in multi-stage CMDP settings. The challenge is that the information of Z is embedded in the states S_t for every time point $t \geq 1$. To infer the counterfactual state $S_t^{Z \leftarrow z'}(\bar{U}_t(H_t))$ at time t , it is necessary to first compute the value of preceding counterfactual state $S_{t-1}^{Z \leftarrow z'}(\bar{U}_{t-1}(H_{t-1}))$ (Line 7, Algorithm 1). This sequential dependency motivates the proposed sequential data preprocessing procedure, where counterfactual states are inferred from $t = 1$ to T .

5.1 Theoretical analysis

In this section, we establish the theoretical results on the regret, which measures the difference between the expected cumulative reward under the optimal policy and that under the estimated policy, and unfairness control of the optimal policy learned using Algorithm 1 and fitted Q iteration (FQI, Riedmiller 2005) in tandem. FQI is widely used policy learning algorithm in RL, where the procedure is detailed in Algorithm 2. Unlike traditional FQI analyses that work on observed states and rewards, our algorithm requires estimating the counterfactual states and rewards before applying FQI. Therefore, this section presents a novel FQI analysis tailored to the scenario where both states and rewards are estimated. For ease of presentation, we use \hat{s} and \hat{r} to represent estimated quantities in theoretical analysis.

Algorithm 2 Fitted Q iteration (Riedmiller 2005).

Input: Dataset $\mathcal{D} = \{(s_i, a_i, r_i, s'_i) : i = 1, \dots, n\}$, function class \mathcal{F} .

- 1: Initialize $\hat{f}_0 \in \mathcal{F}$ randomly.
- 2: **for** $b = 1, \dots, B$ **do**
- 3: Compute target $y_i = r_i + \gamma \max_a \hat{f}_{b-1}(s'_i, a)$.
- 4: Build training dataset $D_b = \{s_i, a_i, y_i\}_{i=1, \dots, n}$.
- 5: Solve a supervised learning problem:

$$\hat{f}_b = \arg \min_{f \in \mathcal{F}} \frac{1}{n} \sum_{i=1}^n (f(s_i, a_i) - y_i)^2$$

- 6: **end for**

Output: Estimated optimal Q function \hat{f}_B .

Here we briefly introduce the assumptions used in the analysis. First, our results are based on the FQI algorithm on the hypothesis class \mathcal{F} that is linear in d -dimensional features $\phi(s, a)$, with bounded coefficients $w \in \mathbb{R}^d$ (Assumption ??). Second, we assume that \mathcal{F} is closed under the Bellman optimality operator (Assumption ??), which is known as the Bellman completeness assumption (Chen & Jiang 2019). Third, we assume sufficient feature coverage in the dataset (Assumption ??). More specifically, we require that the

minimum eigenvalue of $\mathbb{E}_{s,a \sim \mu_b}[\phi(s,a)\phi(s,a)^T]$) is greater than λ_0 where μ_b is the data distribution. This assumption is commonly required to guarantee the convergence of FQI estimators (Wang et al. 2020, Hu et al. 2024). Fourth, we assume that each feature $\phi_i(s,a)$ is a L -Lipschitz continuous function for any $i = 1, \dots, d$ and a (Assumption ??). Fifth, we assume that the reward are bounded, i.e., $|r| \leq R_{\max}$ (Assumption ??). We denote n as the number of experience tuples in the dataset, i.e., $n = NT$.

Theorem 3 (Regret Bound). *Let $\epsilon = \max_s \|\hat{s} - s\|_\infty + \max_r |\hat{r} - r|$. Suppose Assumptions ??-?? holds. With probability at least $1 - n^{-\kappa} - d \exp(-n\lambda_0/8)$ the regret of the optimal policy estimated using Algorithm 1 and FQI is upper bounded by*

$$\frac{CdLR_{\max}\epsilon}{\lambda_0(\lambda_0 - 4dL\epsilon)(1 - \gamma)^3} + \frac{CdR_{\max}\kappa \log(n)}{\lambda_0\sqrt{n}(1 - \gamma)^3} + \frac{\gamma^B R_{\max}}{(1 - \gamma)^2}, \quad (4)$$

for any $\kappa > 0$, some positive constant $C > 0$ and B is the number of FQI iterations.

Theorem 3 implies that the regret bound is composed of three terms: (i) The first term is proportional to ϵ , which measures the *estimation error of counterfactual states and rewards*; (ii) The second term is directly linked to the *one-step FQI regression error*, which approaches zero as n increases; (iii) The third term characterizes the *initialization bias*, which approaches zero exponentially fast with respect to the number of FQI iterations B .

Meanwhile, these error terms are also dependent upon some other factors, such as the feature dimension d , the Lipschitz constant L , the reward upper bound R_{\max} , the minimum eigenvalue λ_0 and the $(1 - \gamma)^{-1}$ -term which has a similar interpretation to the horizon in episodic tasks. Their dependencies align with existing findings in the literature (see e.g., Chen & Jiang 2019, Hu et al. 2024).

To analyze unfairness control of the learned policy, we introduce an additional margin-type assumption, as detailed in Assumption ?? in the supplementary materials. This assumption is often imposed in RL literature (Qian & Murphy 2011, Shi, Zhang, Lu & Song 2022, Hu et al. 2024). Let ξ be the FQI error bound (Equation (??) in the supplementary

materials) and $\hat{\pi}$ denote the learned optimal policy using Algorithm 1 and 2.

Theorem 4 (Unfairness Control). *Under Assumptions ??- ?? and ?? in the supplementary materials, suppose $\epsilon = \max_s \|\hat{s} - s\|_\infty + \max_r |\hat{r} - r|$, for any $\kappa > 0$, with probability at least $1 - n^{-\kappa} - d \exp(-n\lambda_0/8)$, the absolute difference in action distributions for $\hat{\pi}$ using under two counterfactual worlds (z' and z'') is no more than $2^{\alpha+1}\xi^\alpha + 2^\alpha(L\epsilon)^\alpha$.*

Theorem 4 characterizes the difference in action distributions when the input counterfactual states are estimated under two worlds with distinct values of Z . The analysis implies that the unfairness is influenced by two terms: (i) The first term is related to the FQI estimation error. As this error goes smaller, the unfairness also decreases. (ii) The second term is related to the estimation error of counterfactual states. As this estimation error becomes smaller, the estimated counterfactual states under different z 's will be similar, resulting in generating similar action distributions.

6 Numerical experiments

In this section, we evaluate the performance of our approach using synthetic and semi-synthetic datasets that mirror the distributional characteristics of the PowerED study data. Our assessment focused on two key metrics: (1) the value attained by the learned policy, and (2) the degree of counterfactual unfairness. The latter is operationalized as a measure of how actions differ between the observed world and a hypothetical world where only the sensitive attribute is altered.

Baselines Five baselines are considered: 1) *Full*, a standard policy that uses all variables, including the sensitive attribute and other state variables, to make decisions; 2) *Unaware*, a policy that uses all variables except the sensitive attribute to make decisions; and 3) *Oracle*, an idealized policy that used concatenations of counterfactual states where the

counterfactual states and rewards are assumed known. For reference, we also include 4) *Random* policy that selects actions randomly and 5) *Behavior* policy that is used to collect data. By definition, *Random* policies naturally satisfy CF but may not achieve high values.

Fairness metric To measure deviation from counterfactual fairness, we introduce the following CF metric, adapted from previous work (Chen et al. 2023, Wang et al. 2022, Wu et al. 2019),

$$\max_{z', z \in \mathcal{Z}} \frac{1}{NT} \sum_{i=1}^N \sum_{t=1}^T \mathbf{I} \left(A_t^{Z \leftarrow z'}(\bar{U}_t(h_{it})) \neq A_t^{Z \leftarrow z}(\bar{U}_t(h_{it})) \right). \quad (5)$$

This metric calculates the maximum discrepancy between the average discordance rate between actions in the factual and counterfactual worlds across all the time points for any given pair of distinct sensitive attribute values, (z, z') where $z, z' \in \mathcal{Z}, z \neq z'$. A lower value indicates that the policy is fairer. The metric is bounded between 0 and 1, with 0 representing perfect fairness and 1 indicating complete unfairness.

Deployment of our approach: To deploy the learned policy using Algorithm 1 and 2, counterfactual states need to be sequentially estimated. Specifically, before making a decision at time t using \tilde{x}_t , the policy needs to first use the stored \tilde{x}_{t-1} and observed x_t to estimate the value of \tilde{x}_t . Therefore, the learned policy requires a memory buffer to store the counterfactual states at previous time point during deployment.

6.1 Synthetic data experiments

We consider both linear and non-linear transition kernels settings in this experiment. We consider two goals: 1) validate that the level of counterfactual unfairness decreases as the sample size increases for our approach, and 2) investigate how the strength of a sensitive attribute's impact on state and reward affects unfairness. For each setting, we fix the

length of horizon $T = 10$. Let δ denote the strength of impact of sensitive attribute Z on states $\{S_t\}_{t \geq 1}$ and rewards $\{R_t\}_{t \geq 1}$. For the first goal, we vary the sample size N in $\{100, 200, 500, 1000, 2000\}$ and fix δ to be 1. For the second goal, we fix the sample size $N = 1000$ and vary δ in $\{0.0, 0.5, 1.0, 1.5, 2.0\}$. The CF metric is calculated by comparing the action distributions generated by the policy in the observed and corresponding counterfactual world. The cumulative discounted reward is calculated using the observed reward collected from the trajectories. We use $N = 10000$ and $T = 20$ to calculate each metric.

Figure 4(a,b,d,e) present the results for the first goal. As expected, both *Random* and *Oracle* policies achieves prefect CF. The *Full* and *Unaware* policies exhibits high unfairness levels, while our proposed approach achieves lower CF metric. Additionally, the CF metric of our approach decreases with increasing sample size N , validating the consistency. In terms of cumulative discounted reward, the *Full* policy achieves the greatest total reward due to its access to all state information. The other three approaches have lower reward due to the loss of state information, indicating a fairness-reward trade-off (Dutta et al. 2020, Wick et al. 2019). To control the degree of unfairness, a weighted combination of the *Full* policy and our proposed policy could be considered. Greater weight assigned to our proposed method prioritizes fairness, and conversely, greater weight on the *Full* policy prioritizes reward maximization.

Figure 4(c,f) show the results for the second goal. We observe that the unfairness of the *Full* and *Unaware* policies increases with increasing δ , while our proposed approach effectively controls unfairness, indicating that our approach can effectively remove the information of sensitive attribute from the state variables and learn CF policy at varying vulnerabilities to unfairness.

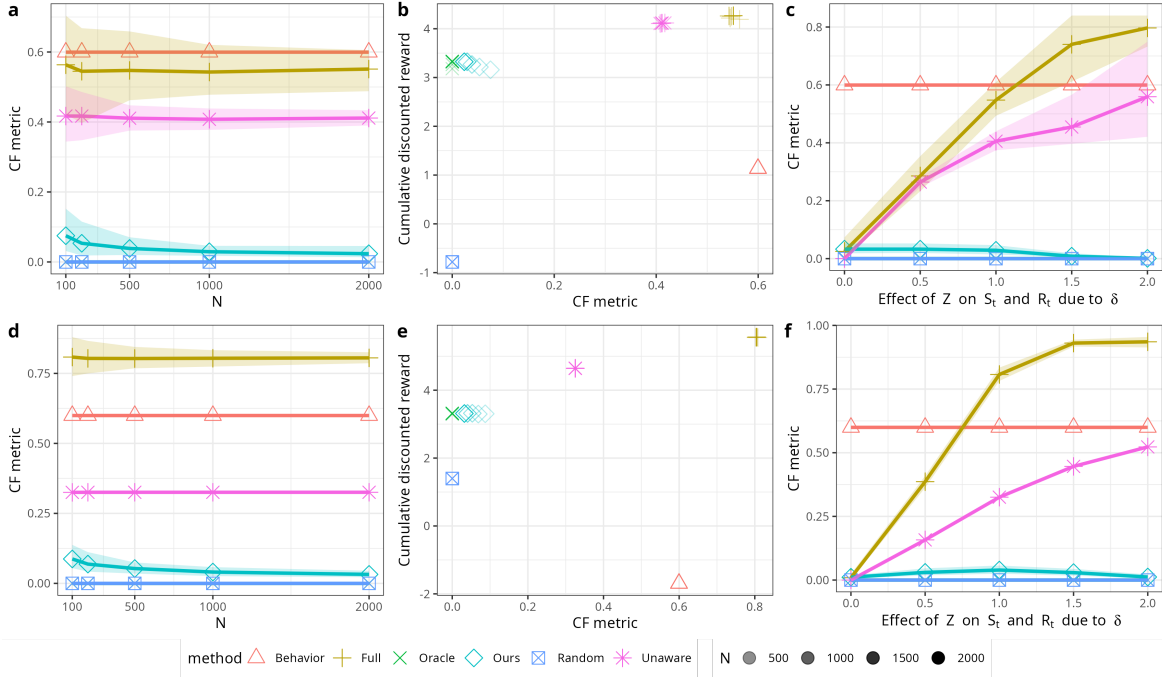


Figure 4: Comparisons under the linear setting (top row) and non-linear setting (bottom row): a,d) CF metric versus sample size, b,e) cumulative discounted reward versus CF metric (multiple sample sizes) with $\delta = 1$, c,f) CF metric versus δ . All the results are aggregated over 100 random seeds. The shaded area represents the 95% CI.

6.2 Semi-synthetic data

To bridge the gap between theoretical results and practical applicability, we conduct real-world data-based simulations to evaluate the performance of different approaches under more realistic conditions. These simulations were designed to mimic the motivating PowerED study (Piette et al. 2023) with respect to transition dynamics. We select education, sex and ethnicity as three different potentially sensitive attributes in our simulations. The state variables include weekly pain intensity score and pain interference score - two commonly used metrics to evaluate progress in pain management programs. The reward is the **7 - weekly self-reported opioid medication risk score**, defined in detail in Piette et al. (2023). We simulate 100 different datasets with $N = 1000$ and $T = 12$ using the neural network-based generative models learned from the real dataset. To investigate how the strength of the sensitive attribute's state variables affects unfairness, we incorporated

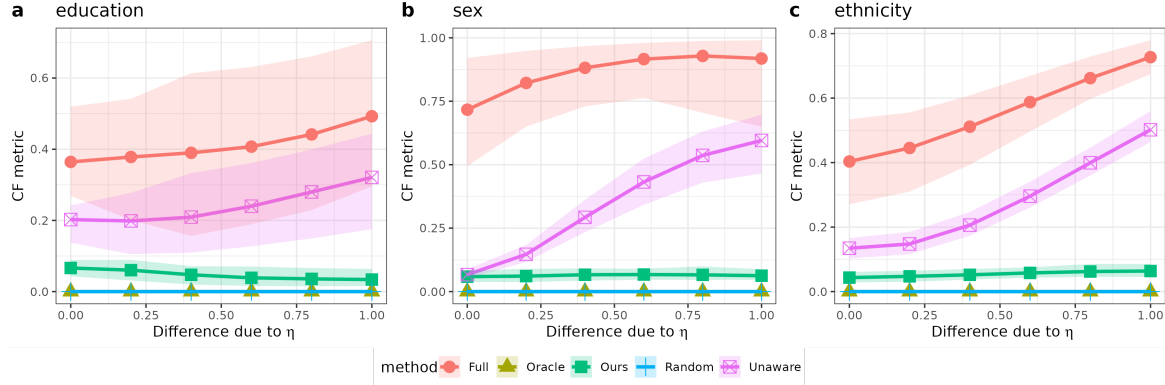


Figure 5: Semi-synthetic experiments: CF metric of different approaches versus η for different sensitive attributes: education, sex, ethnicity. All the results are aggregated over 100 random seeds. The shaded area is the 95% CI.

a strategy similar to the one used in the synthetic data experiments. We varied the effect magnitude of the sensitive attribute on the state variables by adding a constant value η to the state variables for one value of sensitive attribute. The results are shown in Figure 5. We observe that the *Full* policy has high levels of counterfactual unfairness across all scenarios. The *Unaware* policy demonstrates increasing unfairness as the effect of the sensitive attribute on the state variables η increases. This suggests that even after excluding the sensitive attribute, the state variables might still contain residual information of the sensitive attribute, resulting in unfairness. Our proposed approach achieves lower counterfactual unfairness compared with the other two methods. The observed unfairness in our method is primarily due to the approximation error of the counterfactual state when compared with the perfect fairness for the *Oracle* policy. The results are in line with our theoretical findings.

7 Application to Reducing Opioid Misuse Behaviors

In this section, we apply the proposed algorithm to a real-world digital health dataset named PowerED study, as described in Section 1. The data comprise 207 patients over 12 weeks. We selected education, age, gender, and ethnicity as the potentially sensitive

attributes, and weekly pain and pain interference scores as the state variables. The reward is defined as `7 - weekly self-reported opioid medication risk score`, which was measured by items during weekly monitoring calls.

We compare our approach to three baselines: *Full*, *Random* and *Unaware*, as detailed in Section 6. CF metric and cumulative discounted reward are evaluated. To compute the CF metric, we need to assess counterfactual actions under different values of Z , while we only observe a single z in the dataset. Therefore, we train a generative model, similar to the one presented in Section 6.2, to generate counterfactual actions, enabling the calculation of the CF metric. We use fitted Q evaluation (Le et al. 2019) to estimate the value for each policy. The dataset is split into training and validation sets using an 80 : 20 ratio, where the training set is used for policy learning and validation set is used for metric calculations. The results are aggregated for 10 different seeds.

As summarized in Table 1, *Random* policy achieves the perfect fairness but a lower value, as it entirely disregards state information for decision-making. *Full* policy demonstrates the highest value for most variables, however, it has the highest level of unfairness, as incorporating sensitive attributes into the decision-making process can inherently lead to unfair decisions. Our approach achieves the lowest unfairness for all four sensitive attributes compared to other methods. While our approach did not achieve perfect fairness, we believe that the approximation errors associated with estimating counterfactual states and rewards are likely to be relatively higher. Supplemental Figure ?? illustrates the favorability of actions of different policies towards different sensitive groups. It can be seen that the *Full* policy tends to favor younger, more educated, non-Hispanic, and male patients by giving them a higher percentage of treatments compared to other sensitive groups. Our approach mitigates this bias and achieves lower unfairness. Our approach greatly enhanced fair access to human counselors without significantly compromising population-level benefit.

Metric	Method	Education	Age	Sex	Ethnicity
Unfairness	Full	0.44 (0.14)	0.59 (0.15)	0.61 (0.15)	0.39 (0.13)
	Random	0.00 (0.00)	0.00 (0.00)	0.00 (0.00)	0.00 (0.00)
	Unaware	0.10 (0.03)	0.10 (0.02)	0.08 (0.03)	0.21 (0.05)
	Ours	0.06 (0.02)	0.08 (0.02)	0.07 (0.02)	0.16 (0.03)
Value	Full	57.09 (0.31)	57.29 (0.30)	57.20 (0.39)	56.87 (0.33)
	Random	56.61 (0.22)	56.66 (0.27)	56.53 (0.27)	56.54 (0.39)
	Unaware	57.01 (0.18)	57.21 (0.29)	56.96 (0.32)	57.00 (0.31)
	Ours	57.05 (0.30)	57.11 (0.28)	56.95 (0.51)	56.93 (0.48)

Table 1: Unfairness metric (the lower the better) and value (the higher the better) for different approaches in the real data analysis.

8 Discussion

In this paper, we have studied counterfactual fairness in the novel context of RL. We provide a general framework for defining CF in multi-stage settings and theoretically characterize the class of CF policies. We also prove that the optimal CF policy is stationary under stationary CMDPs, which greatly simplifies policy learning. Methodologically, we develop a novel sequential data preprocessing algorithm designed to mitigate bias in multi-stage settings and to produce preprocessed experience tuples to enable learning CF policies by leveraging existing RL methods. We also establish theoretical guarantees on value optimality and unfairness control. Empirical results based on numerical experiments corroborate with our theory. We provide some additional discussions.

Definition 3 Definition 3 extends path-dependent CF (Kusner et al. 2017) to the CMDP setting by fixing the historical action sequence \bar{A}_{t-1} to the observed sequence \bar{a}_{t-1} rather than allowing the past actions to change after switching the value of Z . A direct extension of single-stage CF (Kusner et al. 2017) to CMDP without fixing \bar{A}_{t-1} to \bar{a}_{t-1} would be problematic, as the resulting CF definition would depend on the behavior policy. A further extension to Definition 3 would require action distribution invariance for arbitrary historical action sequences $\bar{a}'_{t-1} \in \mathcal{A}^{t-1}$ that could have but not actually experienced by the individual

in the past (Definition ??, Section ?? in the supplementary materials). The extension requires correcting historical unfair decisions the individual have received before an action at time t , while Definition 3 solely focuses on mitigating decision unfairness at and later than time t assuming past actions \bar{A}_{t-1} cannot be undone. Definition ?? is therefore stricter than Definition 3 and will result in a lower optimal value.

Class of CF Policies We focused on the class of CF policies that takes $(\bar{\mathcal{S}}_t, \bar{\mathcal{R}}_{t-1}, \bar{a}_{t-1})$ as input. Do there exist CF policies outside this class that can achieve higher value? Consider the three policy classes below with increasing restrictiveness. The first class is $\Pi_1 = \{\pi_t : \pi_t(Z, \bar{S}_t, \bar{R}_{t-1}, \bar{A}_{t-1})\}$. DTR (Murphy 2003) ensures that Π_1 contains value-optimal policies, however, direct use of Z violates the CF definition. The second class, $\Pi_2 = \{\pi_t : \pi_t(\bar{\mathcal{S}}_t, \bar{\mathcal{R}}_{t-1}, \bar{A}_{t-1})\}$, removes the information of Z from the policy inputs, which ensures CF but potentially at the cost of reduced value compared to Π_1 . The third class, Π_3 , extends beyond Π_2 by applying do-calculus not only to Z but also to \bar{A}_{t-1} (to any action sequence). While policies in Π_3 satisfy CF, they achieve lower value than those in Π_2 because the information of the observed \bar{A}_{t-1} is removed from policy input.

Additivity Assumption The additive assumption (Assumption 4) can be restrictive in real-world settings. However, it is important to acknowledge that causal inference, especially when dealing with counterfactuals, often relies on strong assumptions (Dawid 2000, Pearl 2009). Relaxing these assumptions may be possible with more flexible approaches, such as variational autoencoder (Louizos et al. 2017) and adversarial training (Melnychuk et al. 2022). We leave this topic for future research.

Supplementary Materials

Supplementary Materials contain a glossary of notation, proofs, supporting figures, tables, longer derivations, and additional results. The following sections are included:

A: Generalization of Definition 3.

B-E: Proofs of Theorems 1 2, 3, 4

F: Details on numerical experiments in Section 6

G: More details on real data analysis in Section 7

Code to reproduce simulations and data analysis will be made available online at github.com.

References

Aghaei, S., Azizi, M. J. & Vayanos, P. (2019), Learning optimal and fair decision trees for non-discriminative decision-making, in ‘Proceedings of the AAAI conference on artificial intelligence’, Vol. 33, pp. 1418–1426.

Barocas, S., Hardt, M. & Narayanan, A. (2023), *Fairness and machine learning: Limitations and opportunities*, MIT Press.

Bennett, A. & Kallus, N. (2024), ‘Proximal reinforcement learning: Efficient off-policy evaluation in partially observed Markov decision processes’, *Operations Research* **72**(3), 1071–1086.

Berk, R., Heidari, H., Jabbari, S., Joseph, M., Kearns, M., Morgenstern, J., Neel, S. & Roth, A. (2017), ‘A convex framework for fair regression’, *arXiv preprint arXiv:1706.02409* .

Beutel, A., Chen, J., Zhao, Z. & Chi, E. H. (2017), ‘Data decisions and theoretical implications when adversarially learning fair representations’, *arXiv:1707.00075* .

Black, E., Elzayn, H., Chouldechova, A., Goldin, J. & Ho, D. (2022), Algorithmic fairness and vertical equity: Income fairness with IRS tax audit models, in ‘Proceedings of the 2022 ACM Conference on Fairness, Accountability, and Transparency’, pp. 1479–1503.

Buçinca, Z., Swaroop, S., Paluch, A. E., Murphy, S. A. & Gajos, K. Z. (2024), ‘Towards optimizing human-centric objectives in ai-assisted decision-making with offline reinforcement learning’, *arXiv preprint arXiv:2403.05911* .

Caton, S. & Haas, C. (2024), ‘Fairness in machine learning: A survey’, *ACM Computing Surveys* **56**(7), 1–38.

Celis, L. E. & Keswani, V. (2019), ‘Improved adversarial learning for fair classification’, *arXiv preprint arXiv:1901.10443* .

Chen, H., Lu, W., Song, R. & Ghosh, P. (2023), ‘On learning and testing of counterfactual fairness through data preprocessing’, *Journal of the American Statistical Association* pp. 1–11.

Chen, J. & Jiang, N. (2019), Information-theoretic considerations in batch reinforcement learning, in ‘International Conference on Machine Learning’, PMLR, pp. 1042–1051.

Chiappa, S. & Isaac, W. S. (2019), ‘A causal Bayesian networks viewpoint on fairness’, *Privacy and Identity Management. Fairness, Accountability, and Transparency in the Age of Big Data. International Summer School, Vienna, Austria, August 20-24, 2018, Revised Selected Papers* 13 pp. 3–20.

Chouldechova, A. (2017), ‘Fair prediction with disparate impact: A study of bias in recidivism prediction instruments’, *Big Data* **5**(2), 153–163.

Chouldechova, A., Benavides-Prado, D., Fialko, O. & Vaithianathan, R. (2018), A case study of algorithm-assisted decision making in child maltreatment hotline screening decisions, in ‘Conference on Fairness, Accountability and Transparency’, PMLR, pp. 134–148.

Corbett-Davies, S., Gaebler, J. D., Nilforoshan, H., Shroff, R. & Goel, S. (2023), ‘The measure and mismeasure of fairness’, *The Journal of Machine Learning Research* **24**(1), 14730–14846.

Creager, E., Madras, D., Pitassi, T. & Zemel, R. (2020), Causal modeling for fairness in

dynamical systems, *in* ‘International Conference on Machine Learning’, PMLR, pp. 2185–2195.

D’Amour, A., Srinivasan, H., Atwood, J., Baljekar, P., Sculley, D. & Halpern, Y. (2020), Fairness is not static: deeper understanding of long term fairness via simulation studies, *in* ‘Proceedings of the 2020 Conference on Fairness, Accountability, and Transparency’, pp. 525–534.

Dawid, A. P. (2000), ‘Causal inference without counterfactuals’, *Journal of the American statistical Association* **95**(450), 407–424.

DeDeo, S. (2014), ‘Wrong side of the tracks: Big data and protected categories’, *arXiv preprint arXiv:1412.4643* .

Di Stefano, P. G., Hickey, J. M. & Vasileiou, V. (2020), ‘Counterfactual fairness: removing direct effects through regularization’, *arXiv preprint arXiv:2002.10774* .

Dutta, S., Wei, D., Yueksel, H., Chen, P.-Y., Liu, S. & Varshney, K. (2020), Is there a trade-off between fairness and accuracy? a perspective using mismatched hypothesis testing, *in* ‘International conference on machine learning’, PMLR, pp. 2803–2813.

Edwards, H. & Storkey, A. (2015), ‘Censoring representations with an adversary’, *arXiv preprint arXiv:1511.05897* .

Hallak, A., Di Castro, D. & Mannor, S. (2015), ‘Contextual markov decision processes’, *arXiv preprint arXiv:1502.02259* .

Hardt, M., Price, E. & Srebro, N. (2016), ‘Equality of opportunity in supervised learning’, *Advances in Neural Information Processing Systems* **29**.

Hébert-Johnson, U., Kim, M., Reingold, O. & Rothblum, G. (2018), Multicalibration: Calibration for the (computationally-identifiable) masses, *in* ‘International Conference on Machine Learning’, PMLR, pp. 1939–1948.

Hollingshead, N. A., Ashburn-Nardo, L., Stewart, J. C. & Hirsh, A. T. (2016), ‘The pain experience of hispanic americans: a critical literature review and conceptual model’, *The*

Journal of Pain **17**(5), 513–528.

Hong, M., Qi, Z. & Xu, Y. (2024), Model-based reinforcement learning for confounded POMDPs, *in* ‘41st International Conference on Machine Learning’.

Howard, A. & Borenstein, J. (2018), ‘The ugly truth about ourselves and our robot creations: the problem of bias and social inequity’, *Science and Engineering Ethics* **24**(5), 1521–1536.

Hu, Y., Kallus, N. & Uehara, M. (2024), ‘Fast rates for the regret of offline reinforcement learning’, *Mathematics of Operations Research* .

Jiang, H. & Nachum, O. (2020), Identifying and correcting label bias in machine learning, *in* ‘International Conference on Artificial Intelligence and Statistics’, PMLR, pp. 702–712.

Kamiran, F. & Calders, T. (2012), ‘Data preprocessing techniques for classification without discrimination’, *Knowledge and Information Systems* **33**(1), 1–33.

Kim, M. P., Ghorbani, A. & Zou, J. (2019), Multiaccuracy: Black-box post-processing for fairness in classification, *in* ‘Proceedings of the 2019 AAAI/ACM Conference on AI, Ethics, and Society’, pp. 247–254.

Kleinberg, J., Ludwig, J., Mullainathan, S. & Rambachan, A. (2018), Algorithmic fairness, *in* ‘Aea papers and proceedings’, Vol. 108, American Economic Association 2014 Broadway, Suite 305, Nashville, TN 37203, pp. 22–27.

Kusner, M. J., Loftus, J., Russell, C. & Silva, R. (2017), ‘Counterfactual fairness’, *Advances in Neural Information Processing Systems* **30**.

Le, H., Voloshin, C. & Yue, Y. (2019), Batch policy learning under constraints, *in* ‘International Conference on Machine Learning’, PMLR, pp. 3703–3712.

Li, M., Shi, C., Wu, Z. & Fryzlewicz, P. (2022), ‘Reinforcement learning in possibly non-stationary environments’, *arXiv preprint arXiv:2203.01707* .

Liu, L. T., Dean, S., Rolf, E., Simchowitz, M. & Hardt, M. (2018), Delayed impact of fair machine learning, *in* ‘International Conference on Machine Learning’, PMLR, pp. 3150–

Louizos, C., Shalit, U., Mooij, J. M., Sontag, D., Zemel, R. & Welling, M. (2017), ‘Causal effect inference with deep latent-variable models’, *Advances in Neural Information Processing Systems* **30**.

Lu, M., Min, Y., Wang, Z. & Yang, Z. (2022), ‘Pessimism in the face of confounders: Provably efficient offline reinforcement learning in partially observable Markov decision processes’, *arXiv preprint arXiv:2205.13589* .

Malibari, N., Katib, I. & Mehmood, R. (2023), ‘Systematic review on reinforcement learning in the field of fintech’, *arXiv preprint arXiv:2305.07466* .

Mehrabi, N., Morstatter, F., Saxena, N., Lerman, K. & Galstyan, A. (2021), ‘A survey on bias and fairness in machine learning’, *ACM Computing Surveys (CSUR)* **54**(6), 1–35.

Melnichuk, V., Frauen, D. & Feuerriegel, S. (2022), Causal transformer for estimating counterfactual outcomes, in ‘International Conference on Machine Learning’, PMLR, pp. 15293–15329.

Murphy, S. A. (2003), ‘Optimal dynamic treatment regimes’, *Journal of the Royal Statistical Society Series B: Statistical Methodology* **65**(2), 331–355.

Nabi, R. & Shpitser, I. (2018), Fair inference on outcomes, in ‘Proceedings of the AAAI Conference on Artificial Intelligence’, Vol. 32.

Pearl, J. (2009), *Causality*, Cambridge University Press.

Pearl, J., Glymour, M. & Jewell, N. P. (2016), *Causal Inference in Statistics: A primer*, John Wiley & Sons.

Pearl, J. et al. (2000), ‘Models, reasoning and inference’, *Cambridge, UK: Cambridge University Press* **19**(2), 3.

Piette, J. D., Thomas, L., Newman, S., Marinec, N., Krauss, J., Chen, J., Wu, Z. & Bohnert, A. S. (2023), ‘An automatically adaptive digital health intervention to decrease opioid-related risk while conserving counselor time: Quantitative analysis of treatment

decisions based on artificial intelligence and patient-reported risk measures', *Journal of Medical Internet Research* **25**, e44165.

Pleiss, G., Raghavan, M., Wu, F., Kleinberg, J. & Weinberger, K. Q. (2017), 'On fairness and calibration', *Advances in Neural Information Processing Systems* **30**.

Puterman, M. L. (2014), *Markov decision processes: discrete stochastic dynamic programming*, John Wiley & Sons.

Qian, M. & Murphy, S. A. (2011), 'Performance guarantees for individualized treatment rules', *Annals of statistics* **39**(2), 1180.

Reuel, A. & Ma, D. (2024), 'Fairness in reinforcement learning: A survey', *arXiv preprint arXiv:2405.06909*.

Riedmiller, M. (2005), Neural fitted q iteration–first experiences with a data efficient neural reinforcement learning method, in 'Machine learning: ECML 2005: 16th European conference on machine learning, Porto, Portugal, October 3-7, 2005. proceedings 16', Springer, pp. 317–328.

Salimi, B., Rodriguez, L., Howe, B. & Suciu, D. (2019), Interventional fairness: Causal database repair for algorithmic fairness, in 'Proceedings of the 2019 International Conference on Management of Data', pp. 793–810.

Shi, C., Uehara, M., Huang, J. & Jiang, N. (2022), A minimax learning approach to off-policy evaluation in confounded partially observable markov decision processes, in 'International Conference on Machine Learning', PMLR, pp. 20057–20094.

Shi, C., Zhang, S., Lu, W. & Song, R. (2022), 'Statistical inference of the value function for reinforcement learning in infinite-horizon settings', *Journal of the Royal Statistical Society Series B: Statistical Methodology* **84**(3), 765–793.

Silva, R. (2024), 'Counterfactual fairness is not demographic parity, and other observations', *arXiv preprint arXiv:2402.02663*.

Sutton, R. S. & Barto, A. G. (2018), *Reinforcement learning: An introduction*, MIT press.

Viviano, D. & Bradic, J. (2024), ‘Fair policy targeting’, *Journal of the American Statistical Association* **119**(545), 730–743.

Wang, H., Ustun, B. & Calmon, F. (2019), Repairing without retraining: Avoiding disparate impact with counterfactual distributions, in ‘International Conference on Machine Learning’, PMLR, pp. 6618–6627.

Wang, R., Foster, D. P. & Kakade, S. M. (2020), ‘What are the statistical limits of offline RL with linear function approximation?’, *arXiv preprint arXiv:2010.11895* .

Wang, Y., Sridhar, D. & Blei, D. (2022), ‘Adjusting machine learning decisions for equal opportunity and counterfactual fairness’, *Transactions on Machine Learning Research* .

Wei, H., Zheng, G., Yao, H. & Li, Z. (2018), Intellilight: A reinforcement learning approach for intelligent traffic light control, in ‘Proceedings of the 24th ACM SIGKDD International Conference on Knowledge Discovery & Data Mining’, pp. 2496–2505.

Wick, M., Tristan, J.-B. et al. (2019), ‘Unlocking fairness: a trade-off revisited’, *Advances in Neural Information Processing Systems* **32**.

Wu, Y., Zhang, L. & Wu, X. (2019), Counterfactual fairness: Unidentification, bound and algorithm, in ‘Proceedings of the Twenty-eighth International Joint Conference on Artificial Intelligence’.

Yang, Y., Lin, M., Zhao, H., Peng, Y., Huang, F. & Lu, Z. (2024), ‘A survey of recent methods for addressing AI fairness and bias in biomedicine’, *arXiv:2402.08250* .

Yeom, S. & Tschantz, M. C. (2018), ‘Discriminative but not discriminatory: A comparison of fairness definitions under different worldviews’, *arXiv preprint arXiv:1808.08619* .

Zuo, A., Wei, S., Liu, T., Han, B., Zhang, K. & Gong, M. (2022), ‘Counterfactual fairness with partially known causal graph’, *Advances in Neural Information Processing Systems* **35**, 1238–1252.

Supplementary Materials for “Counterfactually Fair Reinforcement Learning via Sequential Data Preprocessing”

The supplementary materials contain a glossary of technical notation, a technical extension, proofs of theorems, and additional details about simulation and data analysis.

Contents

A Generalization of Definition 3	2
B Proof of Theorem 1	2
C Proof of Theorem 2	3
D Proof of Theorem 3	5
E Proof of Theorem 4	10
F Details on numerical experiments	12
F.1 Implementation details	12
F.2 Synthetic data	12
F.2.1 Data generating mechanism for linear setting	12
F.2.2 Data generating mechanism for non-linear setting	12
F.3 Semi-synthetic data	13
G More on real data analysis	13

We first provide a glossary for key notation used in the Main Paper.

Symbol	Description
$\bar{S}_t, \bar{A}_t, \bar{R}_t$	historical states, actions and rewards up to time t .
$\bar{U}_t^S, \bar{U}_t^A, \bar{U}_t^R$	historical exogenous variables for states, actions and rewards up to time t .
H_t	$\{Z, \bar{S}_t, \bar{A}_{t-1}, \bar{R}_{t-1}\}$, complete history up to time t
\bar{U}_t	$\{\bar{U}_{t-1}^R, \bar{U}_t^S\}$
$R_{t-1}^{Z \leftarrow z'}(\bar{U}_t(h_t)), S_t^{Z \leftarrow z'}(\bar{U}_t(h_t)), A_t^{Z \leftarrow z'}(\bar{U}_t(h_t))$	the counterfactual reward, state, action that would have been for an individual with history h_t had their sensitive attribute been z' , while experiencing the observed action sequence \bar{a}_{t-1} and following π_t
\mathcal{S}_t	$[S_t^{Z \leftarrow z^{(k)}}(\bar{U}_t(h_t))]_{k=1, \dots, K}$
\mathcal{R}_{t-1}	$[R_{t-1}^{Z \leftarrow z^{(k)}}(\bar{U}_t(h_t))]_{k=1, \dots, K}$

A Generalization of Definition 3

Definition A1 (Strict Counterfactual Fairness in CMDP). *Given an observed trajectory $H_t = h_t$, a decision rule π_t is strictly counterfactually fair at time t if it satisfies the following condition:*

$$\mathbb{P}^{\pi_t} \left(A_t^{Z \leftarrow z', \bar{A}_{t-1} \leftarrow \bar{a}'_{t-1}}(\bar{U}_t(h_t)) = a \right) = \mathbb{P}^{\pi_t} \left(A_t^{Z \leftarrow z, \bar{A}_{t-1} \leftarrow \bar{a}_{t-1}}(\bar{U}_t(h_t)) = a \right), \quad (\text{A.1})$$

for any $z' \in \mathcal{Z}, \bar{a}'_{t-1} \in \mathcal{A}^{t-1}$ and $a \in \mathcal{A}$.

Here the definition is stricter than Definition 3 because it requires action distribution invariance for arbitrary historical action sequences $\bar{a}'_{t-1} \in \mathcal{A}^{t-1}$ that could have but not actually experienced by the individual in the past.

B Proof of Theorem 1

Proof. If we can show that \bar{S}_t, \bar{R}_t and \bar{a}_{t-1} are invariant with respect to the counterfactual values of Z , and given π_t is a function of these quantities, then Equation (3) is invariant to different counterfactual values of Z . **First**, since we fix \bar{A}_{t-1} to be the observed action sequence \bar{a}_{t-1} for all possible values of Z , \bar{a}_{t-1} is invariant to the counterfactual values of Z . **Second**, \mathcal{S}_t consists of the counterfactual states for all possible values of Z . Altering the value of Z does not affect the distribution of \mathcal{S}_t . Since \bar{S}_t is a collection \mathcal{S}'_t for $t' \leq t$, its

distribution of $\bar{\mathcal{S}}_t$ remains invariant to counterfactual values of Z . Similarly, we can show that $\bar{\mathcal{R}}_t$ is invariant to any counterfactual values of Z . As $\bar{\mathcal{S}}_t$, $\bar{\mathcal{R}}_t$ and \bar{a}_{t-1} are invariant with respect to the counterfactual values of Z , any decision rule π_t satisfies Equation (3) is counterfactually fair. \square

C Proof of Theorem 2

Proof. We begin by introducing the following notations

$$\begin{aligned}\mathbb{S}_t^k &= S_t^{Z \leftarrow z^{(k)}} (\bar{U}_t (H_t)), \\ \mathbb{R}_t^k &= R_t^{Z \leftarrow z^{(k)}} (\bar{U}_t (H_t)), \\ \mathbb{S}_t &= \{\mathbb{S}_t^k\}_{k=1,\dots,K}, \\ \mathbb{R}_t &= \{\mathbb{R}_t^k\}_{k=1,\dots,K}.\end{aligned}$$

For simplicity, we include \mathbb{R}_t^k in the set of \mathbb{S}_{t+1}^k . The following conclusions automatically holds if we include U_t^R in the set of U_{t+1}^S . Note that unlike \mathcal{S}_t^k , we do not enforce $\bar{A}_{t-1} \leftarrow \bar{a}_{t-1}$ on \mathbb{S}_t^k . The action sequence \bar{a}_{t-1} can be arbitrary, however, \mathbb{S}_t^k share the same \bar{a}_{t-1} for different k due to Pearl's three-step procedure for counterfactual inference (Pearl et al. 2016). According to Assumption 2, Figure C.1 depicts the relationship between \mathbb{S}_t^k , A_t and U_{X_t} .

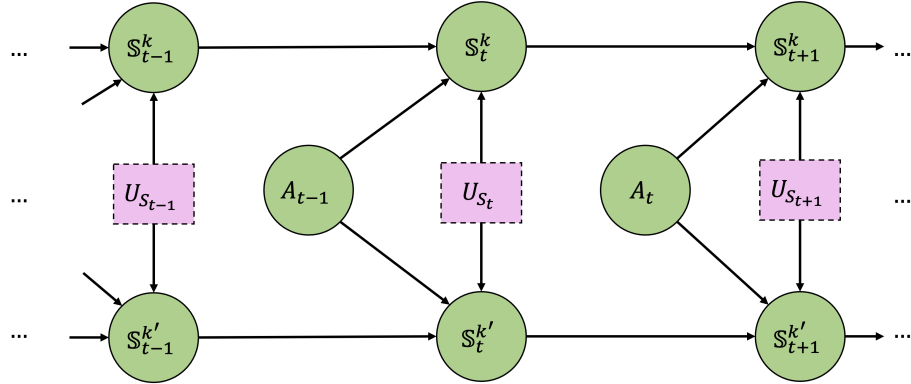


Figure C.1: Causal diagram of counterfactual states and actions.

We have following conclusions via d-separation: for any k

$$\begin{aligned}\mathbb{S}_{t+1}^k &\perp\!\!\!\perp \{\mathbb{S}_j^k, A_j\}_{1 \leq j \leq t-1} \mid \mathbb{S}_t^k, A_t, \\ \mathbb{S}_{t+1}^k &\perp\!\!\!\perp \{\mathbb{S}_j, A_j\}_{1 \leq j \leq t-1} \mid \mathbb{S}_t, A_t.\end{aligned}$$

So far, we have shown that the Markov property holds for \mathbb{X}_t . In the next step, we show the connection between \mathbb{S}_t and \mathcal{S}_t . The key assumption we use here is Assumption 1. We use mathematical induction to show that the Markov property holds for \mathcal{S}_t .

First, assume that for $t \leq l$, we have

$$\begin{aligned}
& P(S_t^{Z \leftarrow z^{(k)}, \bar{A}_{t-1} \leftarrow \bar{a}_{t-1}}(\bar{U}_t(H_t)) \mid S_1^{Z \leftarrow z^{(k)}}(U_1(H_1)), \dots, S_{t-1}^{Z \leftarrow z^{(k)}, \bar{A}_{t-2} \leftarrow \bar{a}_{t-2}}(\bar{U}_{t-1}(H_{t-1}))) \\
& = P(S_t^{Z \leftarrow z^{(k)}}(\bar{U}_t(H_t)) \mid S_{t-1}^{Z \leftarrow z^{(k)}}(\bar{U}_{t-1}(H_{t-1})), A_{t-1} = a_{t-1}) \\
& = P(\mathbb{S}_t^k \mid \mathbb{S}_{t-1}^k, A_{t-1} = a_{t-1}).
\end{aligned} \tag{C.1}$$

It is obvious that **C.1** holds when $t = 2$ due to Assumption 1,

$$\begin{aligned}
& P(S_2^{Z \leftarrow z^{(k)}, A_1 \leftarrow a_1}(\bar{U}_2(H_2)) \mid S_1^{Z \leftarrow z^{(k)}}(U_1(H_1))) \\
& = P(S_2^{Z \leftarrow z^{(k)}}(\bar{U}_2(H_2)) \mid S_1^{Z \leftarrow z^{(k)}}(U_1(H_1)), A_1 = a_1) \\
& = P(\mathbb{S}_2^k \mid \mathbb{S}_1^k, A_1 = a_1).
\end{aligned} \tag{C.2}$$

Second, for $t = l + 1$, we have

$$\begin{aligned}
& P(S_t^{Z \leftarrow z^{(k)}, \bar{A}_{t-1} \leftarrow \bar{a}_{t-1}}(\bar{U}_t(H_t)), \dots, S_1^{Z \leftarrow z^{(k)}, A_1 \leftarrow a_1}(\bar{U}_2(H_2)) \mid S_1^{Z \leftarrow z^{(k)}}(\bar{U}_1(H_1))) \\
& = P(S_t^{Z \leftarrow z^{(k)}, A_2 \dots A_{t-1} \leftarrow a_2 \dots a_{t-1}}(\bar{U}_t(H_t)), \dots, S_2^{Z \leftarrow z^{(k)}}(\bar{U}_{t-1}(H_{t-1})) \mid S_1^{Z \leftarrow z^{(k)}}(\bar{U}_1(H_1)), A_1 = a_1).
\end{aligned} \tag{C.3}$$

Combine **C.3** with **C.2**, we have

$$\begin{aligned}
& P(\{S_j^{Z \leftarrow z^{(k)}, \bar{A}_{j-1} \leftarrow \bar{a}_{j-1}}(\bar{U}_j(H_j))\}_{j=3, \dots, t} \mid S_2^{Z \leftarrow z^{(k)}, A_1 \leftarrow a_1}(\bar{U}_2(H_2)), S_1^{Z \leftarrow z^{(k)}}(\bar{U}_1(H_1))) \\
& = P(\{S_j^{Z \leftarrow z^{(k)}, A_2 \dots A_{j-1} \leftarrow a_2 \dots a_{j-1}}(\bar{U}_j(H_j))\}_{j=3, \dots, t} \mid S_2^{Z \leftarrow z^{(k)}}(\bar{U}_2(H_2)), S_1^{Z \leftarrow z^{(k)}}(\bar{U}_1(H_1)), A_1 = a_1).
\end{aligned} \tag{C.4}$$

By repeating this procedure up to time $t - 1$, we have

$$\begin{aligned}
& P(S_t^{Z \leftarrow z^{(k)}, \bar{A}_{t-1} \leftarrow \bar{a}_{t-1}}(\bar{U}_t(H_t)) \mid \{S_j^{Z \leftarrow z^{(k)}, \bar{A}_{j-1} \leftarrow \bar{a}_{j-1}}(\bar{U}_j(H_j))\}_{j=2, \dots, t-1}, S_1^{Z \leftarrow z^{(k)}}(\bar{U}_1(H_1))) \\
& = P(S_t^{Z \leftarrow z^{(k)}, A_{t-1} \leftarrow a_{t-1}}(\bar{U}_t(H_t)) \mid \{S_j^{Z \leftarrow z^{(k)}}(\bar{U}_j(H_j))\}_{j=2, \dots, t-1}, S_1^{Z \leftarrow z^{(k)}}(\bar{U}_1(H_1)), \bar{A}_{t-2} = \bar{a}_{t-2}) \\
& = P(S_t^{Z \leftarrow z^{(k)}}(\bar{U}_t(H_t)) \mid \{S_j^{Z \leftarrow z^{(k)}}(\bar{U}_j(H_j))\}_{j=2, \dots, t-1}, S_1^{Z \leftarrow z^{(k)}}(\bar{U}_1(H_1)), \bar{A}_{t-1} = \bar{a}_{t-1}) \\
& = P(\mathbb{S}_t^k \mid \{\mathbb{S}_j^k\}_{j=1, \dots, t-1}, \bar{A}_{t-1} = \bar{a}_{t-1}) \\
& = P(\mathbb{S}_t^k \mid \mathbb{S}_j^{t-1}, A_{t-1} = a_{t-1})
\end{aligned} \tag{C.5}$$

The first and second equation are due to Assumption 1, the third equation is due to the Markov property of \mathbb{S}_t^k . Therefore, we show that the Markov property holds for \mathcal{S}_t^k . Similarly, we can show that the Markov property holds for \mathcal{S}_t . Let $\tilde{\mathbb{R}}_t$ to be the weighted sum of \mathbb{R}_t^k ,

$$\tilde{\mathbb{R}}_t = \sum_k p_k \mathbb{R}_t^k,$$

where $\{p_k\}_{k=1, \dots, K}$ are fixed weights with $\sum_k p_k = 1$. Note that we have

$$\mathbb{S}_t, \tilde{\mathbb{R}}_{t-1} \perp\!\!\!\perp \{\tilde{\mathbb{R}}_{j-1}, \mathbb{S}_j, A_j\}_{j=2, \dots, t-2} \mid \mathbb{S}_{t-1}, A_{t-1}.$$

By applying Lemma 1 of (Shi et al. 2020), we show that there exists a stationary deterministic policy $\pi(\cdot|\mathbb{S}_t)$ such that it maximize the integrated value function defined as follow,

$$\begin{aligned}
J(\pi) &= \int_s E \left[\sum_{t=1}^{\infty} \gamma^{t-1} \tilde{\mathbb{R}}_t \mid \mathbb{S}_1 = s \right] P(\mathbb{S}_1 = s) ds \\
&= \int_s E \left[\sum_{t=1}^{\infty} \gamma^{t-1} \sum_k \tilde{\mathbb{R}}_t^k p_k \mid \mathbb{S}_1 = s \right] P(\mathbb{S}_1 = s) ds \\
&= \int_s \sum_k E \left[\sum_{t=1}^{\infty} \gamma^{t-1} \tilde{\mathbb{R}}_t^k \mid \mathbb{S}_1 = s, Z = z_k \right] p_k P(\mathbb{S}_1 = s) ds \\
&= \int_s \sum_k V_0^{\pi}(s, z_k) p_k P(\mathbb{S}_1 = s) ds,
\end{aligned} \tag{C.6}$$

where $V_0^{\pi}(\cdot, \cdot)$ is the value function for original CMDP. Note that we have $\mathbb{S}_1 \perp\!\!\!\perp Z$ due to the definition of counterfactual state. If p_k match the distribution of $P(Z = z_k)$ in the target population, maximizing C.6 is the same as maximizing

$$J_0(\pi) = \int_{s,z} V_0^{\pi}(s, z) P(S_1 = s, Z = z) ds dz,$$

which is the same as integrated value function of original CMDP with observed reward in the target population. \square

D Proof of Theorem 3

Assumption D1 (Hypothesis Class).

$$\mathcal{F} = \{w^T \phi(s, a) : w \in \mathbb{R}^d, \|w\| \leq \mathcal{B}\},$$

where ϕ is a feature map $\mathcal{S} \times \mathcal{A} \rightarrow \mathbb{R}^d$ with $\|\phi(s, a)\|_{\infty} \leq 1$.

Assumption D2 (Completeness). Let \mathcal{T} be the Bellman optimality operator: for $f : \mathcal{S} \times \mathcal{A} \rightarrow \mathbb{R}$,

$$\mathcal{T}f(s, a) = r(s, a) + \gamma \mathbb{E}_{s' \sim P(\cdot|s, a)} \max_{a' \in \mathcal{A}} f(s', a').$$

Assume for any $f \in \mathcal{F}$, $\mathcal{T}f \in \mathcal{F}$.

Assumption D3 (Feature Coverage). There exists a constant $\lambda_0 > 0$ such that

$$\lambda_{\min}(\mathbb{E}_{s,a \sim \mu_b} [\phi(s, a) \phi(s, a)^T]) \geq \lambda_0.$$

Assumption D4 (Lipschitz Continuous Features). There exists a constant $L > 0$ such that

$$\|\phi_i(s, a) - \phi_i(s', a)\| \leq L \|s - s'\|,$$

for any $a \in \mathcal{A}$ and $i = 1, \dots, d$.

Assumption D5 (Bounded Reward). *There exists a constant $R_{\max} > 0$ such that $|r| \leq R_{\max}$.*

Proof. Let w_f denote the parameter estimate when the value function is f , namely,

$$w_f = \left[\sum_{i=1}^n \phi(s_i, a_i) \phi(s_i, a_i)^\top \right]^{-1} \left[\sum_{i=1}^n \phi(s_i, a_i) \left(r_i + \gamma \max_{a' \in \mathcal{A}} f(s'_i, a') \right) \right]. \quad (\text{D.1})$$

Let \hat{w}_f be the corresponding parameter estimate when the s_i , s'_i and r_i are replaced by estimated \hat{s}_i , \hat{s}'_i and \hat{r}_i , namely,

$$\hat{w}_f = \left[\sum_{i=1}^n \phi(\hat{s}_i, a_i) \phi(\hat{s}_i, a_i)^\top \right]^{-1} \left[\sum_{i=1}^n \phi(\hat{s}_i, a_i) \left(\hat{r}_i + \gamma \max_{a' \in \mathcal{A}} f(\hat{s}'_i, a') \right) \right]. \quad (\text{D.2})$$

According to Theorem 8 in [Hu et al. \(2024\)](#), we know that

$$\|Q^* - \hat{f}_B\|_\infty \leq \sum_{t=0}^{B-1} \gamma^t \|\hat{f}_{B-t} - \mathcal{T}\hat{f}_{B-t-1}\|_\infty + \frac{\gamma^B R_{\max}}{1-\gamma}. \quad (\text{D.3})$$

The second term is a diminishing term as the number of iterations B increase. Therefore, we aim to characterize the first term, which is a weighted sum of one-step estimation errors. For any $f \in \mathcal{F}$, one step estimation error can be bounded by,

$$\begin{aligned} \|\hat{w}_f^\top \phi - \mathcal{T}f\|_\infty &\leq \|\hat{w}_f^\top \phi - w_f^\top \phi + w_f^\top \phi - \mathcal{T}f\|_\infty \\ &\leq \|\hat{w}_f^\top \phi - w_f^\top \phi\|_\infty + \|w_f^\top \phi - \mathcal{T}f\|_\infty \\ &\leq \|\hat{w}_f^\top - w_f^\top\|_\infty \cdot \|\phi\|_\infty + \|w_f^\top \phi - \mathcal{T}f\|_\infty. \end{aligned} \quad (\text{D.4})$$

The second term can be bounded by Lemma 7 in [Hu et al. \(2024\)](#). The first term characterizes the estimation error when the state and reward are estimated. To simplify the notation, we denote

$$\begin{aligned} A &= \sum_{i=1}^n \phi(s_i, a_i) \phi(s_i, a_i)^\top, \\ \mathbf{b} &= \sum_{i=1}^n \phi(s_i, a_i) \left(r_i + \gamma \max_{a' \in \mathcal{A}} f(s'_i, a') \right), \\ C &= \sum_{i=1}^n \phi(\hat{s}_i, a_i) \phi(\hat{s}_i, a_i)^\top, \\ \mathbf{d} &= \sum_{i=1}^n \phi(\hat{s}_i, a_i) \left(\hat{r}_i + \gamma \max_{a' \in \mathcal{A}} f(\hat{s}'_i, a') \right). \end{aligned}$$

And we can bound the estimation error,

$$\begin{aligned}
\|\hat{w}_f - w_f\|_\infty &= \|A^{-1}\mathbf{b} - C^{-1}\mathbf{d}\|_\infty \\
&= \|A^{-1}\mathbf{b} - A^{-1}\mathbf{d} + A^{-1}\mathbf{d} - C^{-1}\mathbf{d}\|_\infty \\
&\leq \|A^{-1}\|_2 \|\mathbf{b} - \mathbf{d}\|_\infty + \|A^{-1} - C^{-1}\|_2 \|\mathbf{d}\|_\infty \\
&\leq \|A^{-1}\|_2 \|\mathbf{b} - \mathbf{d}\|_\infty + \|A^{-1}\|_2 \|A - C\|_2 \|C^{-1}\|_2 \|\mathbf{d}\|_\infty. \tag{D.5}
\end{aligned}$$

Next step, we bound each term in (D.5).

Bound $\|A^{-1}\|_2$: By Lemma 7 in Hu et al. (2024), we have

$$P(\lambda_{\min}(A) \geq n\lambda_0/2) \leq d \exp(-n\lambda_0/8).$$

When the event $\lambda_{\min}(A) \geq n\lambda_0/2$ holds, we have

$$\|A^{-1}\|_2 \leq \frac{2}{n\lambda_0}. \tag{D.6}$$

Bound $\|A - C\|_2$: To bound this term, we first consider bounding element-wise difference between A and C ,

$$\begin{aligned}
|A_{jk} - C_{jk}| &= \left| \sum_{i=1}^n \phi_j(s_i, a_i) \phi_k(s_i, a_i) - \phi_j(\hat{s}_i, a_i) \phi_k(\hat{s}_i, a_i) \right| \\
&= \left| \sum_{i=1}^n \phi_j(s_i, a_i) (\phi_k(s_i, a_i) - \phi_k(\hat{s}_i, a_i)) + (\phi_j(s_i, a_i) - \phi_j(\hat{s}_i, a_i)) \phi_k(\hat{s}_i, a_i) \right| \\
&\leq \left| \sum_{i=1}^n (\phi_k(s_i, a_i) - \phi_k(\hat{s}_i, a_i)) + (\phi_j(s_i, a_i) - \phi_j(\hat{s}_i, a_i)) \right| \\
&\leq 2nL\epsilon.
\end{aligned}$$

Therefore, we have

$$\|A - C\|_2 \leq \|A - C\|_F = \sqrt{\sum_{j=1}^d \sum_{k=1}^d |A_{j,k} - C_{j,k}|^2} \leq 2ndL\epsilon \tag{D.7}$$

Bound $\|C^{-1}\|_2$: For any semi positive-definite matrix A and C , we have

$$|\lambda_{\min}(A) - \lambda_{\min}(C)| \leq \|A - C\|_2 \leq 2ndL\epsilon.$$

When the event $\lambda_{\min}(A) \geq n\lambda_0/2$ holds, we have

$$\lambda_{\min}(C) \geq n\lambda_0/2 - 2ndL\epsilon,$$

and we have

$$\|C^{-1}\|_2 \leq \frac{2}{n\lambda_0 - 4ndL\epsilon}. \quad (\text{D.8})$$

Bound $\|\mathbf{b} - \mathbf{d}\|_\infty$: We can bound $\|\mathbf{b} - \mathbf{d}\|_\infty$ by

$$\begin{aligned} \|\mathbf{b} - \mathbf{d}\|_\infty &= \left\| \sum_{i=1}^n \phi(\hat{s}_i, a_i) (r_i + \gamma \max_{a' \in \mathcal{A}} f(s'_i, a'_i) - \hat{r}_i - \gamma \max_{a' \in \mathcal{A}} f(\hat{s}'_i, a'_i)) \right. \\ &\quad \left. + \sum_{i=1}^n (\phi(s_i, a_i) - \phi(\hat{s}_i, a_i)) (r_i + \gamma \max_{a' \in \mathcal{A}} f(s'_i, a'_i)) \right\|_\infty \\ &\leq \left\| \sum_{i=1}^n \phi(\hat{s}_i, a_i) (r_i + \gamma \max_{a' \in \mathcal{A}} f(s'_i, a'_i) - \hat{r}_i - \gamma \max_{a' \in \mathcal{A}} f(\hat{s}'_i, a'_i)) \right\|_\infty \\ &\quad + \left\| \sum_{i=1}^n (\phi(s_i, a_i) - \phi(\hat{s}_i, a_i)) (r_i + \gamma \max_{a' \in \mathcal{A}} f(s'_i, a'_i)) \right\|_\infty \\ &\leq \sum_{i=1}^n |r_i - \hat{r}_i| \left\| \phi(\hat{s}_i, a_i) \right\|_\infty + \gamma \sum_{i=1}^n \left| \max_{a' \in \mathcal{A}} f(s'_i, a'_i) - \max_{a' \in \mathcal{A}} f(\hat{s}'_i, a'_i) \right| \left\| \phi(\hat{s}_i, a_i) \right\|_\infty \\ &\quad + \sum_{i=1}^n \left| (r_i + \gamma \max_{a' \in \mathcal{A}} f(s'_i, a'_i)) \right| \left\| (\phi(s_i, a_i) - \phi(\hat{s}_i, a_i)) \right\|_\infty \\ &\leq \sum_{i=1}^n |r_i - \hat{r}_i| \left\| \phi(\hat{s}_i, a_i) \right\|_\infty + \gamma \sum_{i=1}^n L \|s_i - \hat{s}_i\|_\infty \left\| \phi(\hat{s}_i, a_i) \right\|_\infty \\ &\quad + \sum_{i=1}^n \left| (r_i + \gamma \max_{a' \in \mathcal{A}} f(s'_i, a'_i)) \right| \left\| \phi(s_i, a_i) - \phi(\hat{s}_i, a_i) \right\|_\infty \\ &\leq (1 + \gamma L + \frac{R_{\max} L}{1 - \gamma}) n \epsilon. \end{aligned} \quad (\text{D.9})$$

Bound $\|d\|_\infty$: To bound $\|d\|_\infty$, we consider

$$\begin{aligned} \|d\|_\infty &\leq \|\mathbf{b} - \mathbf{d}\|_\infty + \|\mathbf{b}\|_\infty \\ &\leq (1 + \gamma L + \frac{R_{\max} L}{1 - \gamma}) n \epsilon + \left\| \sum_{i=1}^n \phi(s_i, a_i) \left(r_i + \gamma \max_{a' \in \mathcal{A}} f(s'_i, a') \right) \right\|_\infty \\ &\leq (1 + \gamma L + \frac{R_{\max} L}{1 - \gamma}) n \epsilon + \sum_{i=1}^n \left| \left(r_i + \gamma \max_{a' \in \mathcal{A}} f(s'_i, a') \right) \right| \|\phi(s_i, a_i)\|_\infty \\ &\leq (1 + \gamma L + \frac{R_{\max} L}{1 - \gamma}) n \epsilon + \frac{n R_{\max}}{1 - \gamma}. \end{aligned} \quad (\text{D.10})$$

Bound $\|\hat{w}_f - w_f\|_\infty$: With bound for each term, we have,

$$\begin{aligned}
\|\hat{w}_f - w_f\|_\infty &\leq \|A^{-1}\|_2 \|\mathbf{b} - \mathbf{d}\|_\infty + \|A^{-1}\|_2 \|A - C\|_2 \|C^{-1}\|_2 \|\mathbf{d}\|_\infty \\
&\leq \frac{2}{n\lambda_0} (1 + \gamma L + \frac{R_{\max}L}{1-\gamma}) n\epsilon \\
&+ \frac{2}{n\lambda_0} * 2ndL\epsilon * \frac{2}{n\lambda_0 - 4ndL\epsilon} * ((1 + \gamma L + \frac{R_{\max}L}{1-\gamma}) n\epsilon + \frac{nR_{\max}}{1-\gamma}) \\
&= \frac{2\epsilon}{\lambda_0 - 4dL\epsilon} \left(1 + \gamma L + \frac{R_{\max}L}{1-\gamma}\right) + \frac{8dL\epsilon R_{\max}}{\lambda_0(\lambda_0 - 4dL\epsilon)(1-\gamma)} \\
&\leq C_1 \frac{dLR_{\max}\epsilon}{\lambda_0(\lambda_0 - 4dL\epsilon)(1-\gamma)}, \tag{D.11}
\end{aligned}$$

where we used the fact that $\lambda_0 \leq 1$ and C_1 is a positive constant.

Combined D.11 with Lemma 7 in [Hu et al. \(2024\)](#), we have

$$P \left(\sup_f \|w_f^T \phi - \mathcal{T}f\|_\infty \geq \delta \right) \leq 6d \exp \left(-\frac{\lambda_0^2}{5184d^2(R_{\max} + \mathcal{B})^2} n\delta^2 \right), \tag{D.12}$$

$$P \left(\sup_f \|\hat{w}_f^T \phi - w_f^T \phi\|_\infty \geq \frac{C_1 dLR_{\max}\epsilon}{\lambda_0(\lambda_0 - 4dL\epsilon)(1-\gamma)} \right) \leq d \exp(-n\lambda_0/8). \tag{D.13}$$

Here we assume that there exists a positive constant C^* such that $\mathcal{B} < \frac{C^* R_{\max}}{1-\gamma}$ since the optimal Q function is on the order of $\frac{R_{\max}}{1-\gamma}$ and $\|\phi\|_\infty \leq 1$. We also use the fact that $d < n$. Assume κ is a sufficiently large positive constant, thus we can simplify D.12:

$$P \left(\sup_f \|w_f^T \phi - \mathcal{T}f\|_\infty \geq \frac{C_2 dR_{\max}\kappa \log(n)}{(1-\gamma)\lambda_0\sqrt{n}} \right) \leq n^{-\kappa}, \tag{D.14}$$

where C_2 is a positive constant. Applying Bonferroni inequality to D.13 and D.14, we have

$$P \left(\sup_f \|\hat{w}_f^T \phi - \mathcal{T}f\|_\infty \leq \frac{C_1 dLR_{\max}\epsilon}{\lambda_0(\lambda_0 - 4dL\epsilon)(1-\gamma)} + \frac{C_2 dR_{\max}\kappa \log(n)}{(1-\gamma)\lambda_0\sqrt{n}} \right) \leq 1 - n^{-\kappa} - d \exp(-n\lambda_0/8). \tag{D.15}$$

According to D.3 and Lemma 13 in [Chen & Jiang \(2019\)](#), we have the bound for regret

$$\begin{aligned}
P \left(\nu^* - \nu^{\hat{\pi}_{\hat{f}_B}} \leq \frac{C_1 dLR_{\max}\epsilon}{\lambda_0(\lambda_0 - 4dL\epsilon)(1-\gamma)^3} + \frac{C_2 dR_{\max}\kappa \log(n)}{\lambda_0\sqrt{n}(1-\gamma)^3} + \frac{\gamma^B R_{\max}}{(1-\gamma)^2} \right) \\
\leq 1 - n^{-\kappa} - d \exp(-n\lambda_0/8), \tag{D.16}
\end{aligned}$$

where $\nu^\pi = \mathbb{E}_s^\pi [\sum_{h=1}^\infty \gamma^{h-1} r_h]$. □

E Proof of Theorem 4

Assumption E6 (Margin). *Assume there exist some constants α such that*

$$\mathbb{P} \left\{ s \in S : \max_a Q^{opt}(s, a) - \max_{a' \in A - \arg \max_a Q^{opt}(s, a)} Q^{opt}(s, a') \leq \epsilon \right\} = O(\epsilon^\alpha).$$

where \mathbb{P} is the initial state distribution.

Proof. For each \tilde{s} , we want to derive the bound for $\|\hat{\pi}(\hat{s}_{z'}) - \hat{\pi}(\hat{s}_{z''})\|_2$, where \hat{s}_z is the estimated \tilde{s} when $Z = z$ is observed. Note that by the definition of counterfactuals, the oracle value for $\hat{s}_{z'}$ and $\hat{s}_{z''}$ is \tilde{s} . To simplify the notation, we will omit $\tilde{\cdot}$ in the proof below. By triangle inequality, we have

$$\|\hat{\pi}(\hat{s}_{z'}) - \hat{\pi}(\hat{s}_{z''})\|_2 \leq \|\hat{\pi}(\hat{s}_{z'}) - \hat{\pi}(s)\|_2 + \|\hat{\pi}(s) - \hat{\pi}(\hat{s}_{z''})\|_2. \quad (\text{E.1})$$

The first and second terms in E.1 are similar. Therefore, we only consider the first term in the following proof and another term can be treated similarly. By triangle inequality,

$$\mathbb{E}\|\hat{\pi}(\hat{s}_z) - \hat{\pi}(s)\|_2 \leq \mathbb{E}\|\hat{\pi}(s) - \pi^*(s)\|_2 + \mathbb{E}\|\hat{\pi}(\hat{s}_z) - \pi^*(\hat{s}_z)\| + \mathbb{E}\|\pi^*(\hat{s}_z) - \pi^*(s)\|_2. \quad (\text{E.2})$$

Here we assume that \hat{s}_z and s has the same support S .

Bound $\mathbb{E}_s \|\hat{\pi}(s) - \pi^*(s)\|_2$: Using Theorem 3, we have $P(\mathcal{A}_0) \geq 1 - n^{-\kappa} - d \exp(-n\lambda_0/8)$, where

$$\mathcal{A}_0 = \{\|Q^* - \hat{f}\|_\infty \leq \xi\},$$

where

$$\xi = \frac{C_1 d L R_{\max} \epsilon}{\lambda_0 (\lambda_0 - 4dL\epsilon)(1-\gamma)^2} + \frac{C_2 d R_{\max} \kappa \log(n)}{\lambda_0 \sqrt{n} (1-\gamma)^2} + \frac{\gamma^B R_{\max}}{1-\gamma}. \quad (\text{E.3})$$

For any $s \in S$, suppose

$$\max_a Q^{opt}(s, a) - \max_{a' \in A - \arg \max_a Q^{opt}(s, a)} Q^{opt}(s, a') > 2\xi. \quad (\text{E.4})$$

Under the event defined in \mathcal{A}_0 , we have

$$\max_a \hat{f}(s, a) - \max_{a' \in A - \arg \max_a Q^{opt}(s, a)} \hat{f}(s, a') > 0,$$

and hence

$$\{a \in \mathcal{A} : \hat{\pi}(a|s) = 1\} \subseteq \arg \max_{a \in \mathcal{A}} Q^{opt}(s, a).$$

Thus, we have

$$\|\hat{\pi}(s) - \pi^*(s)\|_2 = 0.$$

Let \mathbb{S} denote the set of s that satisfies equation E.4. It follows that

$$\begin{aligned}
& \int_s \|\hat{\pi}(s) - \pi^*(s)\|_2 \mathbb{I}(\mathcal{A}_0) \mathbb{P}(ds) \\
&= \int_x \|\hat{\pi}(s) - \pi^*(s)\|_2 \mathbb{I}(\mathcal{A}_0) \mathbb{I}(s \in \mathbb{S}^c) \mathbb{P}(ds) \\
&\leq \int_s \mathbb{I}(s \in \mathbb{S}^c) \mathbb{P}(ds) \\
&= (2\xi)^\alpha
\end{aligned} \tag{E.5}$$

Bound $\mathbb{E}\|\hat{\pi}(\hat{s}_z) - \pi^*(\hat{s}_z)\|_2$: Using similar idea for $\mathbb{E}_s\|\hat{\pi}(s) - \pi^*(s)\|_2$, we have

$$\mathbb{E}\|\hat{\pi}(\hat{s}_z) - \pi^*(\hat{s}_z)\|_2 \leq (2\xi)^\alpha \tag{E.6}$$

Bound $\mathbb{E}\|\pi^*(\hat{s}_z) - \pi^*(s)\|_2$: By definition of ϵ , we have $\max_s \|\hat{s}_z - s\| \leq \epsilon$. For any $s \in S$, suppose

$$\max_a Q^{opt}(s, a) - \max_{a' \in A - \arg \max_a Q^{opt}(s, a)} Q^{opt}(s, a') > 2L\epsilon. \tag{E.7}$$

We have

$$\max_a Q^{opt}(\hat{s}_z, a) - \max_{a' \in A - \arg \max_a Q^{opt}(s, a)} Q^{opt}(\hat{s}_z, a') > 0. \tag{E.8}$$

Thus we have

$$\|\pi^*(\hat{s}_z) - \pi^*(s)\|_2 = 0.$$

Let \mathbb{S} denote the set of s that satisfies equation E.7. It follows that

$$\begin{aligned}
& \mathbb{E}_{\hat{s}_z} \left[\int_s \|\pi^*(\hat{s}_z) - \pi^*(s)\|_2 \mathbb{P}(ds) \right] \\
&= \mathbb{E}_{\hat{s}_z} \left[\int_x \|\pi^*(\hat{s}_z) - \pi^*(s)\|_2 \mathbb{I}(s \in \mathbb{S}^c) \mathbb{P}(ds) \right] \\
&\leq \mathbb{E}_{\hat{s}_z} \left[\int_s \mathbb{I}(s \in \mathbb{S}^c) \mathbb{P}(ds) \right] \\
&= (2L\epsilon)^\alpha.
\end{aligned} \tag{E.9}$$

Combined all the results together, we have

$$P \{ \mathbb{E}\|\hat{\pi}(\hat{s}_{z'}) - \hat{\pi}(\hat{s}_{z''})\|_2 \leq 2^{\alpha+1}\xi^\alpha + 2^\alpha(L\epsilon)^\alpha \} \geq 1 - n^{-\kappa} - d \exp(-n\lambda_0/8). \tag{E.10}$$

□

F Details on numerical experiments

F.1 Implementation details

To implement the Algorithm 1, we use a neural network with [64, 64] hidden layer to approximate the transition kernels. The transition kernels are fitted separately for each value of the sensitive attribute to account for potential heterogeneity. Alternative machine learning models can be used to fit the transition kernels depending on the specific characteristics of their data and application domain. The models are fitted using a learning rate of 0.005, a batch size of 512, and a maximum of 1000 epochs. We use the mean squared error as the loss function. To prevent overfitting, the dataset was split into training and testing sets with an 80/20 ratio. Early stopping was implemented to terminate training if the test loss did not improve by more than 0.01 for a consecutive period of 10 epochs. We adopt fitted Q iteration (FQI) algorithm for offline policy learning. The Q-functions are modeled by neural network with a single hidden layer [32]. The FQI algorithm is trained for 100 iterations, and within each iteration, the network was optimized for 500 gradient descent steps using a learning rate of 0.1. The Adam optimizer (Kingma & Ba 2015) is used throughout the experiments. The experiments are conducted on an internal cluster with 60-core Intel Xeon Gold 6230 CPU clocked at 2.10 GHz and 192 GB memory. A discount factor of $\gamma = 0.9$ is used across all experiments.

F.2 Synthetic data

F.2.1 Data generating mechanism for linear setting

$$\begin{aligned} S_1 &= -0.3 + 1.0\delta Z + U_{S_1}, \\ S_t &= -0.3 + 1.0\delta(Z - 0.5) + 0.5S_{t-1} + 0.4(A_{t-1} - 0.5) + 0.3S_{t-1}(A_{t-1} - 0.5) \\ &\quad + 0.3\delta S_{t-1}(Z - 0.5) + 0.4\delta(Z - 0.5)(A_{t-1} - 0.5) + U_{S_t}, \\ R_t &= -0.3 + 0.3S_t + 0.5\delta Z + 0.5A_t + 0.2\delta S_t Z + 0.7S_t A_t - 1.0\delta Z A_t, \end{aligned}$$

where $U_{S_t} \sim \mathcal{N}(0, 1)$, Z takes a binary value in $\{0, 1\}$ with equal probability. Behavior policy is set as $\mathbb{P}(A_t = 1 \mid Z) = \text{expit}(-1.39 + 2.77Z)$. δ is used to control the impact of sensitive attribute on state variables. When $\delta = 0$, the state variables $\{S_t\}_{t \geq 1}$ are independent of sensitive attribute Z ; the effect of Z on $\{S_t\}_{t \geq 1}$ increases as δ increases.

F.2.2 Data generating mechanism for non-linear setting

$$\begin{aligned} S_1 &= -0.7 + 0.8Z + U_{S_1}, \\ S_t &= -1.0 + 0.8\delta Z + 0.25(\sin S_{t-1} + \cos S_{t-1}) + 0.4(A_{t-1} - 0.5) \\ &\quad + 0.15(\sin S_{t-1} + \cos S_{t-1})(A_{t-1} - 0.5) \\ &\quad + 0.15\delta(\sin S_{t-1} + \cos S_{t-1})Z + 0.4\delta Z(A_{t-1} - 0.5) + U_{S_t}, \\ R_t &= -0.2 + 0.3S_t + 0.8\delta Z + 0.8A_t - 0.6\delta S_t Z - 0.7S_t A_t - 1.6\delta Z A_t \end{aligned}$$

where $U_{S_t} \sim \mathcal{N}(0, 1)$, Z takes a binary value in $\{0, 1\}$ with equal probability. Behavior policy is set as $P(A_t = 1 \mid Z) = \text{expit}(-1.39 + 2.77Z)$.

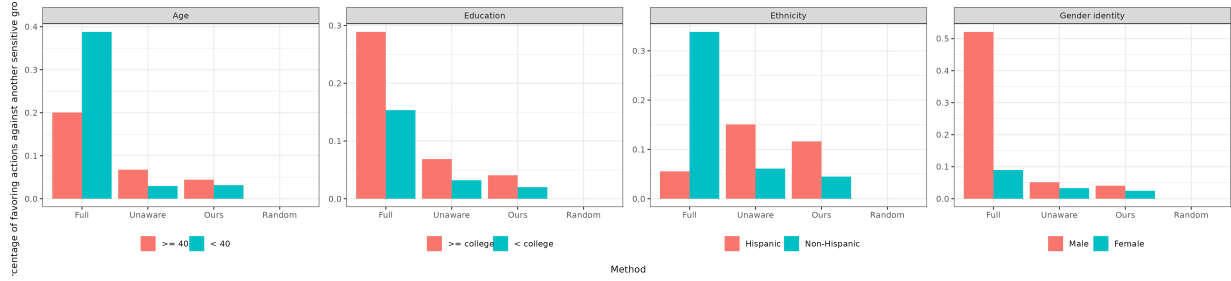


Figure G.2: Percentage of favoring actions against another sensitive groups for age, education, ethnicity and gender identity.

F.3 Semi-synthetic data

To mimic the characteristics of real-world data, we first use the data from PowerED study to learn a generative model. The set of state variables S_t consists of weekly pain score and interference at week t . The reward R_t is defined as the weekly **7 - weekly self-reported opioid medication risk score**. The action A_t is a ternary variable, including a brief motivational interactive voice response (IVR) call (less than 5 minutes), a longer IVR call (5 to 10 minutes), or a live call with counselor (20 minutes). The sensitive attribute is univariate: gender, age, ethnicity, or education. We binarize these sensitive attributes for convenience. In this paper, we choose to focus on the sensitive attributes one at a time instead of multivariate, because the latter, although theoretically possible, makes counterfactual state estimation more challenging given limited sample size. In addition, the univariate approach is standard in the current literature as it isolates the role of each sensitive attribute. To account for potential heterogeneity of transition functions among different sensitive attribute groups, for each sensitive attribute group z , we fit a separate model $P(S_{t+1}, R_t | S_t, A_t, Z = z)$, which follows a multivariate normal distribution with mean $\mu_z(S_t, A_t)$ and diagonal covariance matrix Σ_z . We use a neural network with [32, 32] structure to approximate each $\mu_z(S_t, A_t)$ for $z \in \mathcal{Z}$; the diagonal elements of Σ_z are estimated using the residual variance of each component.

G More on real data analysis

In order to calculate the CF metric for each approach, we use the generative model described in Section 6.2 to generate the states and rewards in the counterfactual world. Please refer to Appendix F.3 for more details on the generative model. Then we apply each method on the factual and counterfactual worlds separately, and calculate the CF metric defined in Section 6. We use fitted Q evaluation (FQE) to evaluate the value for each policy. A neural network with hidden layer [32] is used to model the Q function. The FQE algorithm is trained for 100 iterations, and within each iteration, the network was optimized for 500 gradient descent steps using a learning rate of 0.1. The Adam optimizer is used for optimization.

References

Chen, J. & Jiang, N. (2019), Information-theoretic considerations in batch reinforcement learning, *in* ‘International Conference on Machine Learning’, PMLR, pp. 1042–1051.

Hu, Y., Kallus, N. & Uehara, M. (2024), ‘Fast rates for the regret of offline reinforcement learning’, *Mathematics of Operations Research* .

Kingma, D. P. & Ba, J. (2015), Adam: A method for stochastic optimization, *in* Y. Bengio & Y. LeCun, eds, ‘3rd International Conference on Learning Representations, ICLR 2015’.

Pearl, J., Glymour, M. & Jewell, N. P. (2016), *Causal Inference in Statistics: A primer*, John Wiley & Sons.

Shi, C., Wan, R., Song, R., Lu, W. & Leng, L. (2020), Does the markov decision process fit the data: Testing for the markov property in sequential decision making, *in* ‘International Conference on Machine Learning’, PMLR, pp. 8807–8817.